



Research papers

Estimation of catchment response time using a new automated event-based approach

Eszter D. Nagy^{a,*}, Jozsef Szilagyi^{a,b}, Peter Torma^a

^a Department of Hydraulic and Water Resources Engineering, Faculty of Civil Engineering, Budapest University of Technology and Economics, Műegyetem rkp. 3., H-1111 Budapest, Hungary

^b Conservation and Survey Division, School of Natural Resources, University of Nebraska-Lincoln, Lincoln, Nebraska, USA



ARTICLE INFO

This manuscript was handled by Andras Barossy, Editor-in-Chief

Keywords:

Catchment response time
Time of concentration
Event selection
Detrending moving-average cross-correlation analysis

ABSTRACT

The estimation of catchment response time (T_r) plays an important role in several hydrological and civil engineering design problems. The non-linear relationship between T_r and rainfall intensity necessitates the estimation of an event-based set of T_r values instead of a characteristic constant value. However, there is no generally accepted method to define individual rainfall-runoff events from time-series. Here we propose a new, automated method which results in the selection of rainfall-runoff events and the corresponding T_r values. The proposed method yields an event-based set of T_r values more efficiently than other existing methods and has only two parameters. The results of the new method were compared to those of a statistical and a semi-manual event selection approach. The latter calculates eight different T_r values, including the time of concentration, lag time, time to peak, and time to equilibrium. The median T_r value of the proposed method yields the strongest agreement with the median of the time elapsed between the maxima of the total rainfall and runoff with a root-mean-square error of 4.94 h. It is also demonstrated that a median time of concentration value can be estimated as the maximum of the event based T_r values by the current method. A sensitivity analysis explores the robustness of the proposed method, and also yields the optima of its two parameters. Once calibrated, the present automated methodology dispenses with any event selection procedure.

1. Introduction

Quantification of the catchment response to precipitation via time parameters is essential for engineering tasks, such as peak flow estimation, rainfall-runoff modeling, or flood-risk/environmental hazard mapping. The most frequently used catchment response time (T_r) parameters are the time of concentration (T_c), the lag time (T_L), the time to peak (T_p), and the time to equilibrium (T_e) (Langridge et al., 2020). For example the Rational Method (Chow, 1988) is widely used to estimate the peak flow value to a given precipitation input and requires the calculation of T_c . However, the estimation error of the peak flow value may reach 75 %, due to the uncertainty in the T_c estimates (Bondelid et al., 1982). The response time of a catchment to extreme precipitation limits the time-interval available for flood defense or mitigation of environmental disasters, hence its accurate estimation can also assist in disaster prevention.

Many rainfall-runoff models apply the unit hydrograph theory in some form (Beven, 2012). Therefore, T_c , T_L , and T_p often appear as

model parameters. T_L , in a broader context, is the time between the occurrence of an event and the emergence of a response in the system of interest. The same interpretation of T_L can be used to estimate how long rainfall will take to be translated into runoff in a given catchment (Amiri et al., 2019). T_p is defined as the rise time of a storm hydrograph, encompassing the time from the first stream contributions from a precipitation event to the arrival of the peak flow of the event (Langridge et al., 2020). The International Glossary of Hydrology (WMO, 1974) defines T_c as “the period of time required for storm runoff to flow from the most remote part of a drainage basin to the outlet”. In this definition, “storm runoff” is replaced with “a drop of water”, and “the most remote part” becomes “the furthest point” in many hydrologic texts. However, as Beven (2020) emphasizes, it is not the flow velocities that should be used to define the response times in a catchment, but the relevant surface, subsurface and channel flow celerities or wave velocities. The latter yields the T_e , as it is obtained by integrating the celerity from upslope to a downslope outlet, and can be interpreted as the time from the start of rainfall to peak response (for an initially dry catchment and steady

* Corresponding author.

E-mail address: nagy.eszter@emk.bme.hu (E.D. Nagy).

rainfall, by definition).

Since the publication of Minshall's (1960) classical work on storm runoff from small experimental watersheds, hydrologists agree that the rainfall–runoff response is fundamentally nonlinear (Szilagyi, 2007). Minshall (1960) derived response functions for certain small catchments which showed a pronounced dependence of T_L on the intensity of rainfall excess. The value of T_r was proven to be decreasing with increasing rainfall intensity by many authors since (Reed et al., 1975; Loukas and Quick, 1996; Saghafian et al., 2002; Szilagyi, 2007; Zhang et al., 2007; Kjeldsen et al., 2016; Mathias et al., 2016; Meyersohn, 2016; Michailidi et al., 2018; Cuevas et al., 2019). Therefore, the event-based estimation may be of great use in hydrological applications, such as rainfall-runoff modelling or peak flow estimation. These tasks are especially challenging at ungauged sites, since the value of T_r is usually estimated by empirical formulas. However, the accuracy of empirical equations can be improved with the help of more reliable observed values of T_r .

From studies focusing on time parameter estimation methods, the three main assessment procedures are based on i) measured data; ii) hydraulic equations (Loukas & Quick, 1996; Liang & Melching, 2012; Sabzevari et al., 2015; Baiamonte & Singh, 2016; Michailidi et al., 2018), and; iii) empirical or semi-empirical formulas (Fang et al., 2008; McCuen, 2009; Grimaldi et al., 2012; Nagy et al., 2016; Abdel-Fattah et al., 2017; Kaufmann de Almeida et al., 2017; Ravazzani et al., 2019). Measurements can be made employing i) laboratory models (Black, 1972; Zhang et al., 2007; Liang & Melching, 2012); ii) a tracer substance (Pilgrim, 1976; Azizian, 2019; Björn Rodriguez et al., 2021), or; iii) registering rainfall and runoff data (Loukas & Quick, 1996; McCuen, 2009; Grimaldi et al., 2012; Wu et al., 2016; Gericke & Smithers, 2017; Kaufmann de Almeida et al., 2017; Cuevas et al., 2019; Ravazzani et al., 2019; Langridge et al., 2020; Giani et al., 2021). Tracer measurements can yield detailed information on the runoff generation process of a catchment; however, it is mainly adaptable to small catchments. Such monitoring systems can be operated only for research and not for an operational purpose (Pilgrim, 1976). Nevertheless, only a tracer measurement can be considered as a direct measurement of T_r . The results obtained by employing laboratory models are not necessarily valid for natural catchments (Gaál et al., 2012). Due to the above mentioned applicability issues of tracer measurements and laboratory models, the present authors chose to estimate the observed value of T_r indirectly from recorded rainfall and runoff data.

The main disadvantages of calculating T_r using observed rainfall and runoff time-series are i) difficulties with event selection, and; ii) the

assessment of time instants on the hyeto- and hydrographs that require the separation of effective precipitation and direct runoff.

The event selection can be performed manually, but this task is quite cumbersome and hard to reproduce, especially in the case of a large dataset (Thiesen et al., 2019). Several of the automated event selection methods rely on base flow separation (e.g., Merz & Blöschl, 2009; Mei & Anagnostou, 2015; Tarasova et al., 2018). The main disadvantage of these methods is that base flow is an elusive process to quantify compared to other components of the water balance, such as precipitation and total runoff (Szilagyi et al., 2003). The true value of the base flow is usually unknown therefore its value can never be precisely quantified from just rainfall-runoff records. Additionally, these event selection methods may involve empirical estimation of parameters further reducing objectivity, while other methods, relying on machine learning, require training. Table 1 lists some recently published automated event selection methods with their weaknesses explained.

Considering the attributes of the available event selection approaches, the statistical method of Fischer et al. (2021) appeared to be the most appropriate to compare the event-selection capability of the proposed technique. Additionally, a method requiring expert knowledge (from here on referred to as the semi-manual method) and involves visual screening of the selected events is also employed in conjunction with the present one in order to ensure a base set of regular hyeto- and hydrographs for the estimation of T_r .

Once the events are selected, the 'observed' value of T_r can be derived for each event from temporal differences between specific time instants on the hyeto- and hydrographs via so-called graphical definitions. Although the study of response-time parameters dates back more than 150 years, their definition and calculation are still intricate tasks. Time parameters cannot be uniquely identified due to their various interpretations. This is underlined by the existence of numerous graphical definitions for T_c in the literature. McCuen (2009), for example, lists six definitions of T_c , out of which one is a definition of T_p , and two are definitions of T_L . Even the most often used definition has two slightly different versions, namely the time from the end or center of mass of rainfall excess to the end of direct runoff (i.e., the inflection point on the total runoff hydrograph). Coincidentally, Giani et al. (2021) recently published a novel method to estimate T_r relatively easily and objectively from observed time-series.

The new methodology called Detrending Moving-average Cross-correlation Analysis (DMCA) introduced by Giani et al. (2021) greatly facilitates the calculation of T_r . It allows the user to estimate the characteristic value of T_r from long time-series while making possible the

Table 1
State-of-the-art automated event selection methods.

Reference	Events/ catchment/year	Catchment area [km ²]	Region of study	Temporal resolution	Method applied	Disadvantage(s)
Khanal (2004)	0.715	unknown	Texas, USA	unknown	Semi-automatic, based on unit hydrograph method.	Manual extraction of multi-peaked events and events with unwanted shapes.
Merz & Blöschl, (2009)	7.02	5–10000	Austria	Hourly	Automated, based on several criteria.	Requires base flow separation.
Norbiato et al., (2009)	2.55	7.3–608.4	Italian Alps	Hourly	Same as in Merz & Blöschl (2009).	Same as in Merz & Blöschl (2009).
Koskelo et al. (2012)	64.8	14–293	Mid-Atlantic Region of North America	Daily	Sliding Average with Rain Record (SARR) method.	Restricted to small basins and coarse (daily) temporal resolution.
Mei & Anagnostou (2015)	9.11	400–5900	North Carolina, USA	Hourly	Automated, physical basis.	Only for basins with a clear recession period. Requires base flow separation.
Tarasova et al. (2018)	19.1	31–23700	Germany	Daily	Automated, based on several criteria.	Requires base flow separation.
Thiesen et al. (2019)	19.7	113	Alps, Austria	Hourly	Data-driven method, based on information theory.	Only tested on one catchment. Requires a high amount of training data. Selects only runoff events.
Oppel & Mewes (2020)	1.5–2.9	10–1400	Germany	Hourly	Machine learning.	No code published. Requires training and employs only discharge data.
Fischer et al. (2021)	2.98	3–26000	Germany	Daily	Statistical analysis of long time-series.	Employs nine parameters. Hourly temporal resolution was tested only on one catchment.

estimation of T_r at the event scale, using pre-defined subsections of the observed data for specific events. For performing the latter, event selection must be done separately and beforehand. The event selection approach applied by Giani et al. (2021) is automated, but includes the empirical estimation of T_L and a screening criterion regarding peak flow magnitude.

The present authors aim to extend the DMCA-based T_r estimation method of Giani et al. (2021) by performing the event selection and estimation of a set of T_r values for the selected events simultaneously. This is achieved by introducing an additional parameter. From here on the currently proposed method is to be referred to as ‘event-scale DMCA’ or shortly, ‘E-DMCA’ method. Consequently, the study presented in this paper has three main foci:

- I. Validating the applicability of the proposed event-scale DMCA-based T_r estimation method for accurate event selection by comparing the results of the new approach with the results of a state-of-the-art, statistical and an expert-knowledge-based, semi-manual event selection method.
- II. Assessing the robustness and validity of the proposed range of the two parameters needed to perform the event-scale DMCA-based T_r estimation method by performing a thorough sensitivity analysis.
- III. Exploring the relationship between the event-based T_r values resulting from the often-used graphical definitions and the event-scale DMCA-based T_r estimation.

Toward the first goal, we performed the previously mentioned semi-manual event selection (see Section 3.1) and assessed the value of T_r from each event by applying eight different graphical definitions collected from literature. Then, the new event-scale DMCA-based T_r estimation method was applied (see Section 3.3), which concurrently performs the event selection and the calculation of T_r using the DMCA-based method of Giani et al. (2021), obliterating the need for external event selection required by the DMCA-based T_r estimation method. Next, the statistics-based event selection method of Fischer et al. (2021) was evaluated to provide a comparative basis for the event selection capability of the proposed event-scale DMCA-based method (see Section 3.2). The results of the three methods were compared in terms of the event selection and T_r values (see Sections 4.1 and 4.2, respectively). The sensitivity analysis mentioned in II is introduced in Section 3.4, while its results are presented in Section 4.3. A discussion on the performance of the event-scale DMCA-based T_r estimation method is provided in Section 5, including a more detailed comparison of the T_r values

given by the graphical definitions and those obtained by the proposed method. The conclusions of the present study are found in Section 6.

Similar to Giani et al. (2021), the term of catchment response time (T_r) is employed throughout the text in general and the other time parameters (T_c , T_L , T_p , and T_e) are specified only when it is theoretically plausible. In what follows, the method presented by Giani et al. (2021) is referred to as the ‘DMCA-based T_r estimation (DMCA) method’, while the approach presented in this paper is called the ‘event-scale DMCA-based T_r estimation (E-DMCA) method’ or ‘proposed method’. The two event selection methods for testing the E-DMCA results are referred to as the ‘semi-manual event selection (SM) method’ and the ‘statistics-based automated flood event separation (SBES) method’.

2. Study area and data

In this study, 61 small- to medium-sized Hungarian catchments, six of them nested, were examined. Fig. 1 provides an overview of the catchments’ location, while relevant statistical measures are given in Table 2. The list of catchments is provided in Supplementary Material S1. The catchment IDs appearing throughout the text correspond to the ones presented in Supplementary Material S1. The mean catchment area is 206 km², from a range of 8.74–810 km². 54 % of the catchments are smaller than 150 km², and 6.5 % have an area larger than 500 km². Based on the high-resolution Copernicus land-use/land-cover products (Copernicus, 2020a; Copernicus, 2020b), the minimum forest coverage is 3.8 %, the maximum is 88.7 %, while the range of impervious area is 0.3–19.9 %. A third of the catchments are located within karst regions. The dominant soil parent types are deposits: glacial and alluvial, loess and loess-like, tertiary, and older deposits. Volcanic rocks, such as andesite, rhyolite, and basalt, dominate only in a few (<5%) catchments, while sandstone, shale, and phyllite cover even fewer catchments. According to the Köppen climate classification (Peel et al., 2007), Hungary’s climate is predominantly warm-summer humid continental. The time window of the study extends from 2000 to 2017. During this period, the minimum amount of annual rainfall and catchment runoff were 394 and 21.1 mm, respectively, while the maxima were 1377 and 642 mm. The aridity index varies between 0.75 and 1.25 among the catchments.

The catchments were delineated using the Copernicus Land Monitoring Services’ EU-DEM v1.1 digital surface model, a freely available raster format dataset with a spatial resolution of 25 m (Copernicus, 2016). High-resolution (5 min) discharge and precipitation time-series were provided by the local Water Directorates for 64 and 17 stations, respectively. Observed discharge were derived using measured water

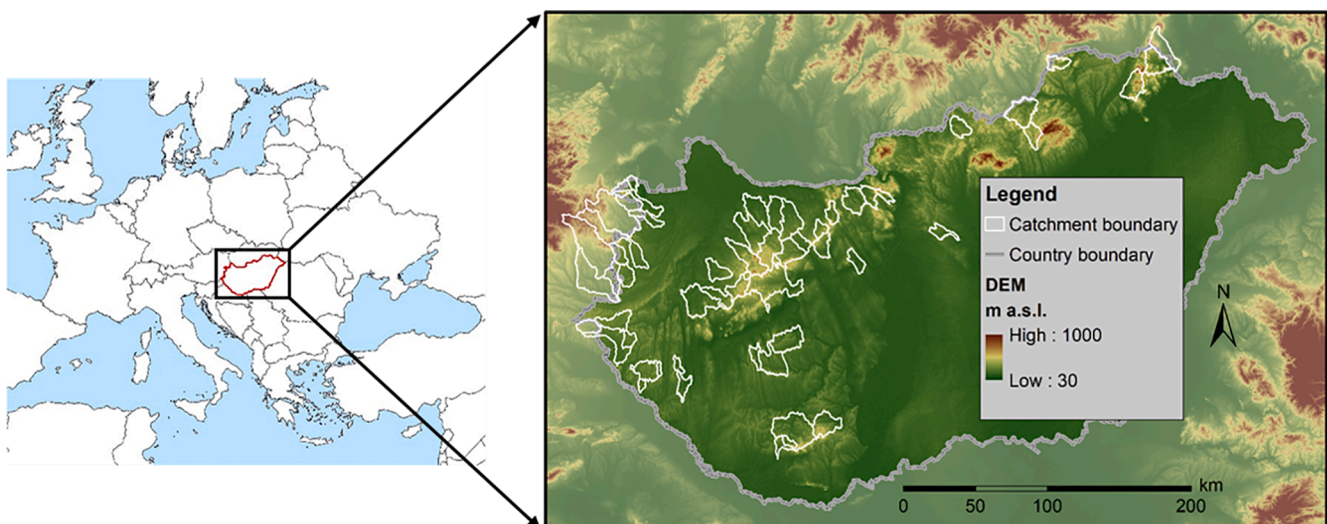


Fig. 1. Overview of the study area and catchments.

Table 2
Minimum, maximum, and mean values of the important catchment descriptors.

	Catchment area [km ²]	Longest flowpath [km]	Elevation [m a.s.l.]	Mean slope of watershed [%]	Highest stream order (Strahler, 1957) [-]	Ratio of impervious surfaces [%]	Ratio of forests [%]	Annual runoff [mm]	Annual precipitation [mm]	Aridity index [-]
Minimum	8.74	5.08	103	1.1	2	0.3	3.8	21.1	394	0.75
Maximum	810	88.3	1629	22.2	5	19.9	88.7	642	1377	1.25
Mean	206	32.9	264	9.7	4	8.9	69.4	74.6	756	1.10

levels and rating curves. The three main catchment selection criteria applied were i) no considerable human influence on flow; ii) high temporal resolution of measurements, and; iii) continuous record available for at least ten years (similar to [Sauquet & Catalogne, 2011](#)). The first criterion was ensured by checking digital maps and consulting the local water directorates. Not every catchment has a rainfall gauging station near or in the catchment, and sub-daily precipitation data is not provided by the Hungarian Meteorological Service free-of-charge to obtain interpolated values. The 17 precipitation gauging stations operated by the local water directorates do not cover the whole study area, therefore they could not be used to interpolate precipitation data. Instead, European Centre of Medium-Range Weather Forecast (ECMWF) re-analysis data from the Copernicus Climate Data Store were used in addition to the gauging station values. For catchments without a gauging station, ECMWF data were used. The Era5 Land product ([Copernicus Climate Change Service, 2019](#)) provides hourly precipitation time-series with a $0.1^\circ \times 0.1^\circ$ ($\sim 9 \text{ km} \times 9 \text{ km}$) spatial resolution. The applicability of the ECMWF re-analysis data was examined separately in a previous study by [Nagy & Szilagyi \(2020\)](#) where the results of the SM approach (see [Section 3.1](#) for details) employing measured and also re-analysis data were compared at 38 catchments having (or the closest assigned) a precipitation gauging station. We found that the ECMWF data is adequate for T_r estimation, especially when the centers of masses and also, peaks of the observed runoff and rainfall time-series are used.

3. Methodology

3.1. Calculating catchment response time for events – SM method

During a previous study ([Nagy & Szilagyi, 2021](#)), eight graphical definitions of T_r were collected and analyzed. The interpretation of definitions a)-h) is presented in [Fig. 2](#). Definition a) is the most often

used, i.e., conventional definition of T_c and definition b) is a slightly different version of the latter, however, definition a) is much more often used. Definitions e) and f) are infrequently used, i.e., unconventional interpretations of T_c reported by [McCuen \(2009\)](#), not used for any other time parameter (i.e., T_L , T_p , or T_e). Both definitions c) and d) stand for T_L , even though only definition d) is correct by the unit hydrograph theory ([Chow, 1988](#)). Definition g) represents T_p and definition h) is the T_e . Unfortunately, all definitions can be found in the literature as the definition of T_c ([Wisnovszky, 1958](#); [Loukas & Quick, 1996](#); [McCuen, 2009](#)).

Most of the definitions [a)-e) and g)] require the separation of base flow and/or effective precipitation. In this study, the former was performed using a recursive filtering method ([Nathan & McMahon, 1990](#)). The latter was calculated by assuming a constant-rate loss and equaling the direct runoff and excess rainfall volumes, known as the Φ -index method ([Dingman, 2015](#)). This way, only one parameter had to be adjusted: the coefficient of the recursive filter. It was manually calibrated for every catchment using the ten largest runoff events resulting from steps i)-ii) (see below), and validated for the smaller events. The aim of the calibration procedure (by a trial and error fashion) was to find a coefficient for each watershed that ensures the temporal coincidence of the end of the direct runoff and the inflection point on the recession limb. The latter was identified visually on the hydrographs. After the separations, all eight graphical definitions were calculated.

The initial data set consisted of 64 catchments and 7189 events. After quality control and screening (see steps i)-vi) below), 2152 events remained for 61 catchments. For these events, the observed values of T_r were derived by the eight definitions presented in [Fig. 2](#). The number of events per watershed ranges from 11 to 69. On average, 35 events were available for a catchment. The runoff event identification and screening procedure included the following steps:

- i) First, the peak flows were found in the streamflow time-series. Only peaks from the snow-free period (April 1 until October

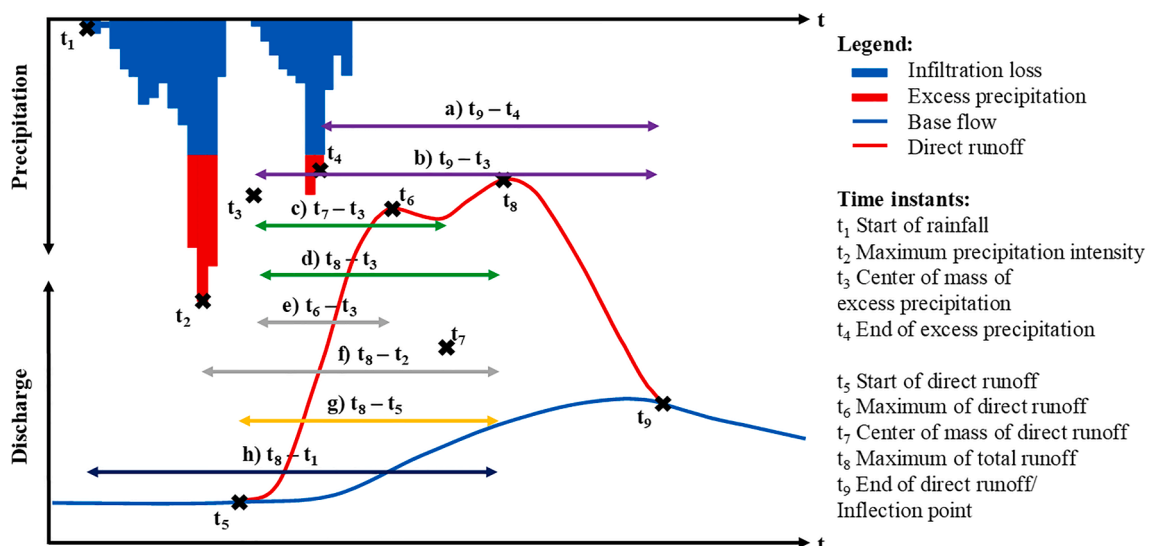


Fig. 2. Graphical definitions of T_r most frequently occurring in the literature. Color codes: purple – conventional T_c ; green – T_c and T_L ; grey – unconventional T_c ; yellow – T_c and T_p ; navy blue – T_c and T_e . (For interpretation of the references to color in this figure legend, the reader is referred to the web version of this article.)

- 31) were selected, with a value higher than double the long-term mean flow. The beginning and the end of runoff events were found as the first time instant when base flow reached 90 % of the total flow before and after the peak, respectively. Applying this approach, 7189 events were collected and sorted in the decreasing order of peaks for 64 catchments automatically.
- ii) The selected events were then screened manually in order to provide a base set of regular hydrographs. These consist of a clear rising and falling limb, but can have multiple peaks. Events with unwanted shapes [e.g., having oscillating discharge (i.e., discharge changing continuously and periodically between two values, indicating measurement error of the water level), a long constant discharge segment, linearly increasing/decreasing segments, etc.] were identified visually and removed from the set of events, reducing the number of events by 61.5 %. The two main reasons causing an unwanted hydrograph shape were identified as measurement errors and missing measurements.
 - iii) Next, the precipitation event related to each runoff event had to be determined. First, the algorithm found the beginning of the precipitation event as the first non-zero value before the start of direct runoff. Second, it defined the end of the precipitation event by searching for the last non zero value after the peak flow.
 - iv) After the separation of direct runoff and effective precipitation (employing a recursive filter and the Φ -index method, respectively), events with insufficient rainfall were dropped, causing a further 7.0 % loss of events.
 - v) Three catchments were excluded from the dataset having less than ten events. The number of events dropped by 0.2 %.
 - vi) After defining the necessary characteristic points on the hydro- and hietographs, all eight definitions were calculated. Events producing negative T_r values were excluded, which meant another 1.4 % reduction, ending up with a total of 2152 events for the 61 catchments.

3.2. Comparison of the event selection methods – SBES method

The adequacy of the E-DMCA method in terms of event selection was demonstrated by comparing with one of the state-of-the-art event separation methods. However, no objectively verifiable rainfall-runoff event separation exists, therefore, an objective evaluation of the proposed method is not possible. The statistics-based automated flood event separation (SBES) method of Fischer et al. (2021) was chosen for a comparison with the E-DMCA and SM methods. The main reasons for selecting this method were its i) reproducibility due to the freely available R package; ii) applicability for hourly time-series; iii) suitability to select both runoff and the corresponding rainfall events, and; iv) convertibility to select not only floods, but also smaller runoff events. However, the SBES method was only tested for one catchment at an hourly temporal resolution by Fischer et al. (2021). As they state, their “method should not be easily transferred from daily to hourly values because of the different behavior of the runoff data.”

Fischer et al. (2021) published recommended values for the nine parameters employed by the SBES method, however, these values were calibrated to select flood events from daily time-series. The parameters are:

- The window for the moving variance of the 1-day (or 1-hour) discharge differences d_{var} . This parameter is generally catchment-dependent and can be chosen based on catchment size. The present authors used a single constant value for every catchment similar to Fischer et al. (2021).
- The parameter for the variance threshold θ . A smaller θ leads to the selection of more events, therefore, it can be used to adjust the number of events selected per year if desired.
- The three thresholds for defining the start of the flood event, η , γ and κ . Parameter η provides a threshold for the relative 1-day (or 1-hour)

discharge difference for the flood event to start. Parameter κ controls the level of significant contribution a pre-flood has to have to be part of the flood event. If there is an increase in magnitude in excess of $\kappa\%$ of the total peak within $\gamma + 1$ days before the flood event, this “pre-flood” is included in the flood event. The parameter γ can be also chosen according to catchment size and climate region of the catchment.

- Two parameters δ and ω to specify the end of the flood event. To find the end of the events, two criteria are compared. First, it is checked if the baseflow level at the start of the event is reached again. Second, it inspects whether the next ω time steps after the potential end of the flood event would add less than δ of the discharge volume of the falling limb if they were included. If either of these criteria are met, the end of the event is found.
- The parameter d_{dur} to specify a time window for superpositioned flood events. An extraordinary duration of a separated flood event with multiple peaks becomes an indicator for a series of superimposed flood events. The parameter d_{dur} can be chosen according to the catchment size and the climatic conditions.
- For the separation of the flood-inducing precipitation, the buffer b had to be defined by parameter ξ , where ξ is the minimum time lag between the start of precipitation and ensuing flood event. Its value can also depend on catchment size.

The parameter values suggested by Fischer et al. (2021) include $d_{var} = 3$, $\theta = 0.25$, $\eta = 0.1$, $\gamma = 1$, $\kappa = 0.4$, $\delta = 0.2$, $\omega = 2$, $d_{dur} = 40$. They also found, that $d_{var} = 14.5$ and $\theta = 0.33$ were suitable parameter values for the hourly resolution at their selected test catchment. Since the E-DMCA and SM methods identify not only floods but also runoff events, the present authors aimed to find a parameter set for the SBES method which also yields runoff events. This was achieved by lowering the value of θ to 0.01. The value of η was also reduced to 0.01, since neither 0.25 nor 0.33 produced acceptable starting points for the runoff events.

Another modification was made by the present authors regarding the identification of the corresponding precipitation. The original script appeared to run for hours for one catchment due to the high number of fitted linear regressions. Regression fitting is computationally expensive, therefore the present authors optimized the script and ran it on a shorter section of the data. The results of the optimized script were checked for one catchment to ensure the agreement between the results of the original and the optimized code. This way, the runtime was reduced from days to hours for the 61 catchments examined in this study.

3.3. Calculating catchment response time for events – DMCA and E-DMCA methods

Giani et al. (2021) successfully applied the DMCA method to directly estimate characteristic T_r from rainfall and streamflow observations. As they state, this method’s strength is “to find the timescale at which two time-series are linked even when they exhibit different frequency spectra and are nonlinearly related”. The DMCA-based correlation coefficient (ρ_{DMCA} [-]) for time-series with length T and applying a window length L can be calculated as:

$$\rho_{DMCA}(L) = \frac{\sum_{t=0.5(L+1)}^{T-0.5(L-1)} (R_t - \widehat{R}_{t,L})(Q_t - \widehat{Q}_{t,L})}{\sqrt{\sum_{t=0.5(L+1)}^{T-0.5(L-1)} (R_t - \widehat{R}_{t,L})^2 \sum_{t=0.5(L+1)}^{T-0.5(L-1)} (Q_t - \widehat{Q}_{t,L})^2}} \text{ with } -1 \leq \rho_{DMCA}(L) \leq 1 \quad (1)$$

where R_t and Q_t are the cumulative time-series of the rainfall (r) and streamflow (q) data, while $\widehat{R}_{t,L}$ and $\widehat{Q}_{t,L}$ are the centered moving averages of the cumulative rainfall and streamflow time-series, given as:

$$R_t = \sum_{i=1}^t r_i, Q_t = \sum_{i=1}^t q_i \text{ for } t = 1, 2, \dots, T \quad (2-3)$$

$$\widehat{R}_{i,L} = \frac{1}{L} \sum_{t=-0.5(L-1)}^{i+0.5(L-1)} R_t \widehat{Q}_{i,L} = \frac{1}{L} \sum_{t=-0.5(L-1)}^{i+0.5(L-1)} Q_t \quad (4-5)$$

The rainfall and streamflow time-series must have the same length and temporal resolution. This study employed hourly time-series, similar to Giani et al. (2021). The window length L must be defined in units of time steps (in this case, hours) and must have an odd value since a centered moving average is calculated. The value of T_r can be estimated as half of $L_{min}-1$, where L_{min} is the window length resulting in the minimum value of ρ_{DMCA} (ρ_{min} [-]). In order to find this optimum, several window lengths need to be applied. The maximum possible value of T_r ($T_{r,max}$ [hr]) can be attributed to the maximum tested window length (L_{max} [hr]). This L_{max} value can be considered as the only parameter of this approach. This parameter limits the maximum value of T_r as $(L_{max} - 1) / 2 = T_{r,max}$.

The numerator in Equation (1) represents the bivariate fluctuation of streamflow and runoff, while the denominator contains the squared fluctuations of the rainfall and streamflow time-series. The sign of the rainfall and streamflow fluctuations carries physical meaning: the center of mass is preceded by a negative fluctuation and followed by a positive one (Giani et al., 2021). Therefore, ρ_{min} is achieved when the value of L is closest to the time between the centers of masses. A detailed, step-by-step introduction to the DMCA method is presented by Giani et al. (2021), along with a detailed description of the calculation steps' interpretation.

The proposed E-DMCA method takes advantage of the fluctuations mentioned above, by introducing a new parameter, p_{th} [-]. The DMCA method applied to the whole time-series results in a single, characteristic value of T_r ($T_{r,char}$). Using the time window (L_{min}) attributed to this characteristic T_r and relying on the cumulative rainfall and streamflow time-series' fluctuations, rainfall-runoff events are expected to be located at sections having positive rainfall and negative streamflow fluctuations. These sections can be found by applying a threshold value (p_{th}), as a new parameter. Based on this hypothesis, the steps of event selection and T_r calculation were defined as follows:

- i) Estimating the characteristic T_r and the corresponding value of L_{min} using the DMCA method of Giani et al. (2021) on the entire time-series.
- ii) Normalizing the rainfall and streamflow fluctuation time-series [$N_{rain}(L_{min})$ and $N_{flow}(L_{min})$] attributed to L_{min} . The normalization of the fluctuation time-series is only performed to facilitate data comparison and visualization, but it does not affect the result of the event selection.
- iii) Finding the time instants in the normalized fluctuation time-series, where rainfall fluctuations are higher than $1 - p_{th}$ and streamflow fluctuations are lower than the p_{th} threshold value. The threshold value is defined as a percentile of the entire normalized fluctuation time-series $N_{flow}(L_{min})$ and $N_{rain}(L_{min})$. The selection criteria can be written as: $\{p[N_{rain}(L_{min})] > 1-p_{th}\} \wedge \{p[N_{flow}(L_{min})] < p_{th}\}$, where p [-] represents percentiles. The time instants meeting the criteria form continuous sections of consecutive time steps.
- iv) Selecting the first time instant (i.e., the beginning of the events) for each continuous section identified in step iii).
- v) Calculating the value of T_r for each event ($T_{r,event}$) with the DMCA method. The time window for each event starts $T_{r,max}$ hours before the first time instant and ends two times $T_{r,max}$ hours after the first time instant.
- vi) Excluding ill-conditioned events with $\rho_{min} \geq 0$ and with $T_{r,event} = T_{r,max}$. (See further explanation below.)
- vii) Removing outliers from the final set of event-based values. Outliers were defined as elements in excess of triple the scaled median absolute deviation from the median of the original set of values.

The interpretation of these steps is visualized in Fig. 3 for sections of real data. Step i) utilizes the DMCA method presented by Giani et al. (2021). Steps ii)-iv) build on the outcome ($T_{r,char}$ or L_{min}) of step i) to perform the event selection. Since both the original and normalized fluctuation time-series follow a symmetric distribution, the event selection threshold (p_{th}) was defined as percentiles in step iii). This way, the event selection criteria are adjusted to the characteristics of the rainfall and streamflow time-series for each catchment. Step iii) results in continuous sections where the threshold criteria are met. In step iv), every first time instant of these sections will be selected as the start of the event. The time windows had to be fitted to each starting point in the next step. These time windows specify the beginning and endpoints of the time-periods for which the DMCA method is applied again, separately for every event. The length of the time window was selected based on the rule of thumb applied in the unit hydrograph method (see step v) above), since the base of the triangular unit response hydrograph is often described in relation to T_r (FEH, Institute of Hydrology, 1999). This way, a set of T_r values ($T_{r,event}$) can be retrieved from the whole time-series for each watershed. Please note that in steps i)-v) the event selection and T_r estimation for every event is performed.

In step vi) and vii), some of the inadequate values are removed from $T_{r,event}$. Ill-conditioned events consist of rainfall and runoff time-series the DMCA method yields inadequate T_r values with. Events resulting in a positive value of ρ_{min} are not necessarily unacceptable, but it was found that a positive coefficient indicates ill-conditioned events in most cases. Events resulting in T_r values equivalent of $T_{r,max}$ may also be ill-conditioned or have longer T_r than $T_{r,max}$. Therefore, these values were also excluded. An example of $\rho_{min} \geq 0$ and another for $T_{r,event} = T_{r,max}$ can be seen in Fig. 3, along with an example of a well-conditioned event. The ratio of ill-conditioned events ranged between 0 and 3.18 % and 1.93–2.96 %, respectively. The filtered outliers made 0–1.16 % of the initially selected events. The strengths and weaknesses of the presented event selection method are discussed in more detail in Section 4.1. The Matlab function of the E-DMCA method (Nagy, 2022) is available at <https://doi.org/10.5281/zenodo.6822134>.

3.4. Sensitivity analysis and goodness-of-fit measures

The E-DMCA method has two parameters a) the maximum value of T_r [$T_{r,max} = (L_{max} - 1) / 2$], and; b) the threshold value of fluctuations identifying events (p_{th}). A sensitivity analysis was carried out to assess the robustness of the proposed method. During this analysis, a wide range of the two parameters were tested (see Section 4.3 for results). The consistency of the sensitivity analysis was ensured by a twofold cross-validation approach. The sensitivity analysis was performed for two subsets of the catchments of equal number. The catchments were sorted into the subsets randomly. The goodness-of-fit was measured between the median of $T_{r,event}$, and the median of definition f), as the DMCA method tends to match the maxima of the rainfall and streamflow time-series (for details, see Section 5.2).

During the sensitivity analysis and comparison of the results of event selection methods, the following goodness-of-fit measures were applied: Pearson correlation coefficient (r [-]), Nash-Sutcliffe efficiency (NSE [-]) (Nash & Sutcliffe, 1970), root-mean-squared error ($RMSE$ [hr]) and the sum of relative differences (ΔT_r [%]). These were calculated as:

$$r = \frac{\sum_{i=1}^n (x_i - \bar{x})(y_i - \bar{y})}{\sqrt{\sum_{i=1}^n (x_i - \bar{x})^2 \sum_{i=1}^n (y_i - \bar{y})^2}} \quad (6)$$

$$NSE = 1 - \frac{\sum_{i=1}^n (y_i - x_i)^2}{\sum_{i=1}^n (x_i - \bar{x})^2} \quad (7)$$

$$RMSE = \sqrt{\frac{\sum_{i=1}^n (y_i - x_i)^2}{n}} \quad (8)$$

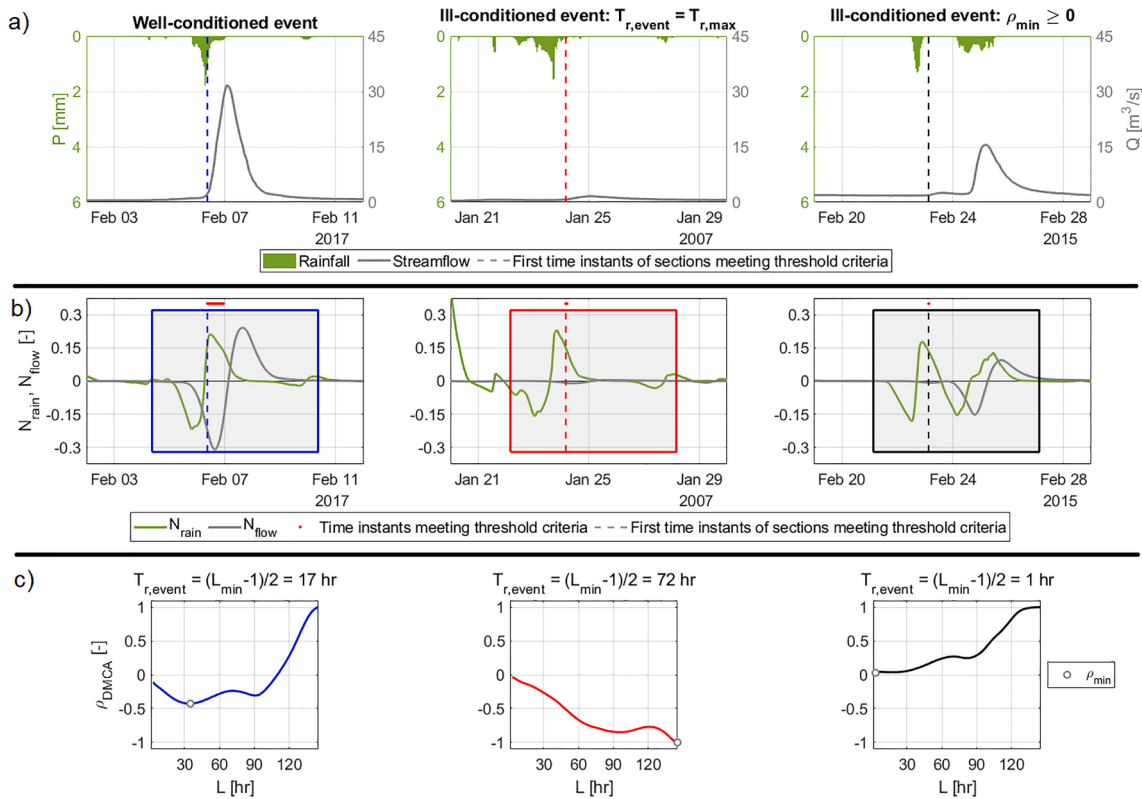


Fig. 3. Examples for a well-conditioned event (blue), and the two types of ill-conditioned events $\rho_{min} \geq 0$ (red) and $T_{r,event} = T_{r,max}$ (black) which yield inadequate T_r values with the E-DMCA method. a) Streamflow (Q) and rainfall (P) time-series with the first time instants of sections. b) The normalized fluctuation time-series of rainfall and precipitation (N_{rain} , N_{flow}) with the time instants and event windows. c) DMCA-based correlation coefficient related to window length [$\rho_{DMCA}(L)$]. (For interpretation of the references to color in this figure legend, the reader is referred to the web version of this article.)

$$\Delta T_r = \frac{\sum_{i=1}^n y_i - x_i}{\sum_{i=1}^n x_i} 100 \quad (9)$$

where x_i is the value of T_r yielded by the baseline (SM or SBES) method, y_i is the value of T_r resulting from the E-DMCA method, and n is the number of observations. The value of r can range from -1 to 1 , meaning perfect inverse linear and linear relationship, respectively. The value of NSE shows the model's capability of yielding a better estimate than the mean of the observed values, and its value can range from $-\infty$ to 1 . If NSE is in the range of $0-1$, the model provides a better estimation than the observed values' mean. An NSE value of 1 represents a perfect fit. The $RMSE$ value is zero for a perfect fit, and the lower the value the better is the fit. The value of ΔT_r defines the fit's estimation error in percentage relative to the observed values. A negative ΔT_r implies a general underestimation of the observed values. A value of 0 does not represent a perfect fit, it only means that there is no significant under- or overestimation.

4. Results

4.1. Comparison of event characteristics from different selection methods

The three methods selected different sets of events and as a result the statistical characteristics of various parameters may considerably differ. Although, the three methods cannot be compared objectively based on the number of events, we provide the number of selected events per catchment per year for each event selection method in [Supplementary Material S2, Section 3](#). The largest number of events is obtained by the E-DMCA method, followed by the SBES, and the SM, respectively. The lowest number by SM is due to the discharge threshold and the visual inspection when any disturbed runoff event was rejected (step i. and ii. in [Section 3.1](#)).

In order to compare the event selection capability of the E-DMCA approach, the runoff ratio (α [-]) and the value of T_r was assessed for every event selected by the SM, E-DMCA, and SBES methods. The runoff ratio was calculated as the ratio of the total runoff and the total precipitation, while T_r was calculated using the DMCA method for each subsection of rainfall and runoff data. [Figs. 4 and 5](#) present the different percentiles of the calculated T_r and α values for every selected event. [Sections 1 and 2 in Supplementary Material S2](#) includes more details separately for every percentile, including plots for all events and only matched events.

The value of T_r demonstrates a stronger correlation between the results of the E-DMCA and the SBES methods than the E-DMCA and the SM methods. The middle range of the values ($p = 0.25, 0.5$, and 0.75) is captured well, while the low and high values ($p = 0.1$ and 0.9) less so. Both E-DMCA and SBES methods result in slightly smaller T_r values than the SM one. In contrast, E-DMCA shows considerably less scatter than SBES when they are compared to SM. Considering the α values, the best agreement is obtained between SM and E-DMCA. Not only the variation of the median values from the SBES method ($\sigma_{0.5} = 3.20 \cdot 10^{-3}$) is higher than that either from the E-DMCA ($\sigma_{0.5} = 6.04 \cdot 10^{-4}$) or SM ($\sigma_{0.5} = 7.59 \cdot 10^{-4}$) method, but also the deviation from the 1:1 line. The SBES method shows remarkable under- and overestimations in the range of $0.02-0.09$ against both the SM and E-DMCA methods. We highlight that the runoff ratio is explicitly checked only in the case of the expert-based SM method during the event selection procedure. The median values of α yielded by the SBES method are higher on average than of the E-DMCA method. The interpretation of these results is given in [Section 5.1](#).

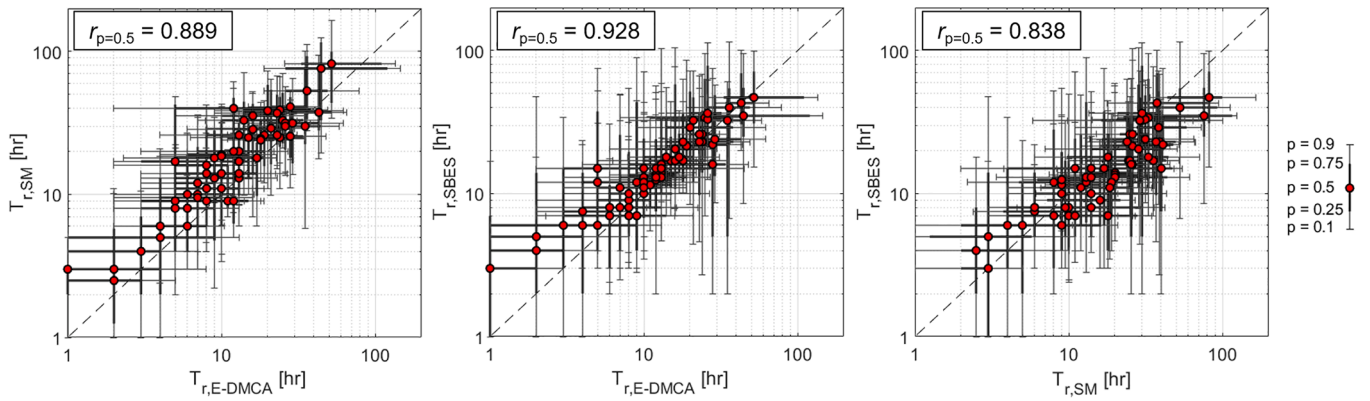


Fig. 4. Comparison of the different percentiles ($p = 0.1, 0.25, 0.5, 0.75, 0.9$) of T_r resulting from the E-DMCA ($T_{r,E-DMCA}$) against those from the SBES ($T_{r,SBES}$) and SM ($T_{r,SM}$) methods.

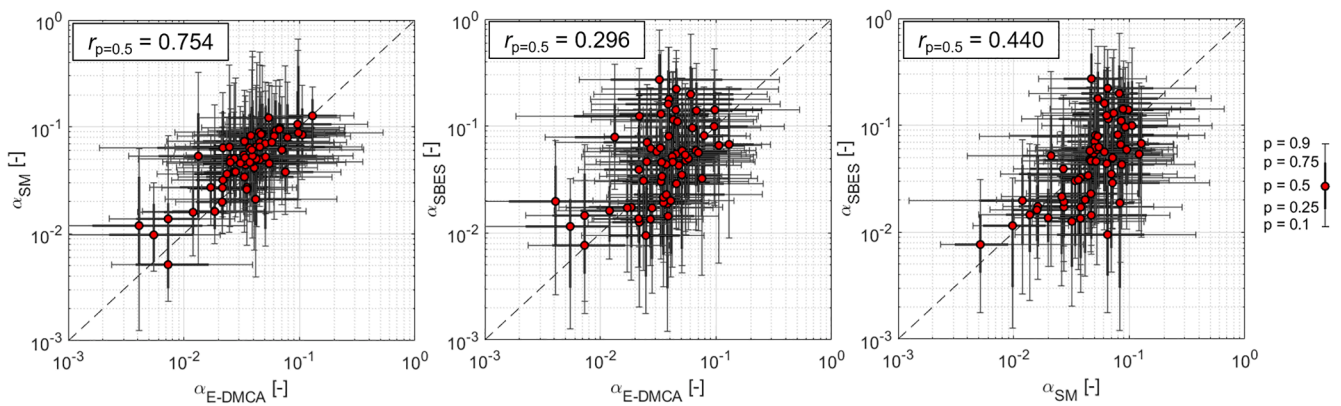


Fig. 5. Comparison of the different percentiles ($p = 0.1, 0.25, 0.5, 0.75, 0.9$) of α resulting from the E-DMCA (α_{E-DMCA}) against those from the SBES (α_{SBES}) and SM (α_{SM}) methods.

4.2. Comparison of the catchment response time values resulting from different methods

The SM event selection resulted in eight different T_r values – according to the definitions shown in Fig. 2 – for the 61 catchments’ 2152

events. Another set of event-based values ($T_{r,event}$) for each catchment was provided by the E-DMCA method, while the original DMCA method gave a characteristic T_r ($T_{r,char}$) value for the whole time-series. The final results were obtained by employing $T_{r,max} = 150$ h and $p_{th} = 0.05$, based on the sensitivity analysis results (see Section 4.3). The difference

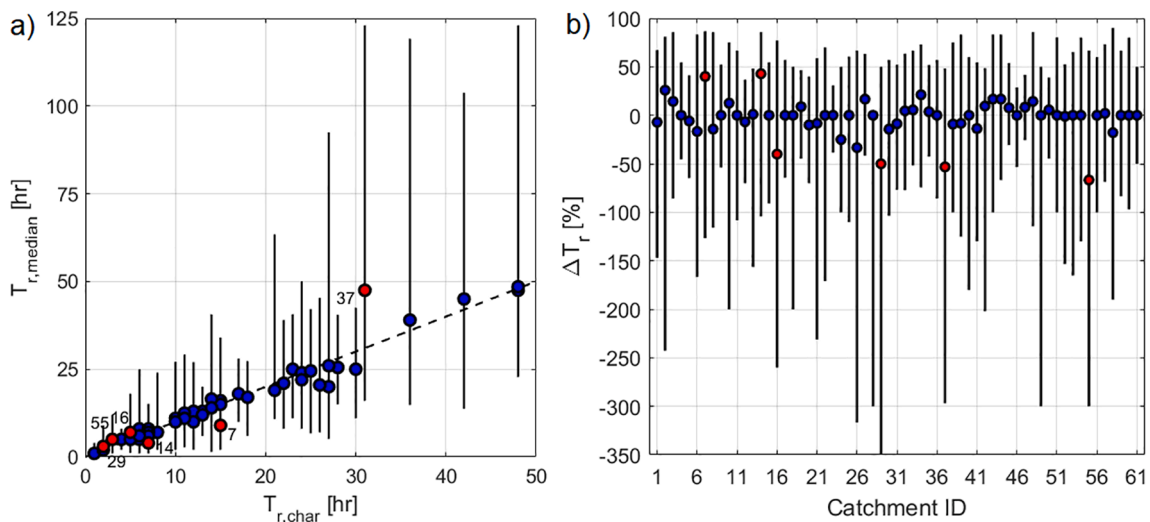


Fig. 6. a) Medians (filled circles) of the event-based values ($T_{r,median}$) from the E-DMCA method plotted against the characteristic T_r values ($T_{r,char}$) by the DMCA method. b) The difference between $T_{r,char}$ and $T_{r,median}$ expressed in percentage for each watershed. Catchments with relative error higher than 40% are marked in red. The whiskers span the 0.05–0.95 percentile range. Catchment IDs correspond to the ones presented in Supplementary Material S1. (For interpretation of the references to color in this figure legend, the reader is referred to the web version of this article.)

between the characteristic value ($T_{r,char}$) obtained by the DMCA method and the median of the values ($T_{r,median}$) resulting from the E-DMCA method is presented in Fig. 6.

The characteristic T_r shows good agreement with $T_{r,median}$ having a Pearson correlation of 0.967 and Nash-Sutcliffe coefficient of 0.935. The difference is equal to or higher than 40 % in six watersheds (shown by red markers), which is ~ 10 % of the total number of catchments. The difference is only 1–3 h in the case of four watersheds (14, 16, 29, 55), which have a smaller area and, therefore, a smaller T_r . In one case (37), the flow may be distorted by measurement errors yielding irregular N_{flow} curves. In this case, the E-DMCA method captures a fewer number of events than the SM method. The proposed method appears to capture a higher number of the smaller peaks and fewer large ones at catchment 7, therefore yields a shorter response time than the characteristic T_r . Nevertheless, 85 % of the watersheds has an error < 20 %.

In case of the SM event selection, all eight definitions (see Fig. 2) were applied for each event. The median values from each definition were compared to the medians ($T_{r,median}$) of the E-DMCA method both considering every selected events and only those selected by both methods in Fig. 7. The goodness-of-fit measures described in Section 3.4 were also calculated (Table 3). A figure (Figure S4) similar to Fig. 7 is provided in Supplementary Material S2 comparing the values yielded by the combination of the SBES and DMCA methods and the values resulting from the different definitions.

The median of the eight different T_r definitions gave diverse results. The two traditional definitions of T_c [a) and b)] resulted in the highest values, followed by the medians of T_e and T_p [definitions g) and h)]. The remaining four definitions yielded similar values. From these four, definitions e) and d) (standing for T_L), and definitions f) and c) (the two unconventional definitions of T_c) expressed the best agreement with the values of $T_{r,median}$, respectively. The match is the closest to the 1:1 line in case of definition f), which is the time elapsed between the peaks of total rainfall and streamflow. The four best-performing definitions resulted in NSE values higher than 0.8 and $RMSE$ values under 6.2 h. ΔT_r shows negative values in every case, which means that $T_{r,median}$ somewhat underestimates the values resulting from the different definitions. This

estimation error ranges two orders of magnitude, and the smallest value is over -1% . The absolute value of ΔT_r is under 2 % for definitions d)-f).

As the E-DMCA procedure appeared to capture the median of definition f), it is instructive to compare the distributions of the event-based values resulting from the SM and the proposed method for this definition. Therefore, the values representing the $p = 0.1, 0.25, 0.5, 0.75$ and 0.9 percentiles ($p = 0.5$ being the median) were compared. The plots of the five percentiles can be seen in Fig. 8. The goodness-of-fit measures for each percentile can be found in Table 4. For a better comparison, the different percentiles are also plotted for the events selected by both methods in Fig. 8. In Table 4, the corresponding goodness-of-fit measures are also provided in parentheses.

The different percentiles of the E-DMCA method gave satisfactory results overall. The percentile plot is generally symmetric along the 1:1 line and the length of the whiskers are similar in most cases (see Fig. 8). The value of NSE is 0.708 on average, while the value of r exceeds 0.875 in every case. $RMSE$ shows a considerable increase as the estimated percentile increases. The increase of error is expected since the range of the estimated values also increases. However, the relative error varies: the $p = 0.1$ and 0.75 percentiles are over-, while the other percentiles are underestimated. The largest relative error is somewhat higher than 10 % in the case of the largest values ($p = 0.9$). As it appears in Fig. 8, the E-DMCA values tend to overestimate the larger values and underestimate the lower ones in case of the higher percentiles ($p = 0.75$ and 0.9).

4.3. Sensitivity analysis

The results of the sensitivity analysis introduced in Section 3.4 are presented in Fig. 9. The event selection was performed using the parameter value ranges of $p_{th} = 0, 0.01, 0.025, 0.05, 0.1, 0.25, 0.4, 0.5$ and $T_{r,max}$ values from 50 to 350 hr, incremented by 25 hr. Note that $p_{th} = 0$ results in the selection of no events, and $p_{th} = 0.5$ results in selecting every possible event due to the symmetry of the rainfall and flow fluctuation distributions. $T_{r,max} = 0$ hr also results in the selection of no events. Therefore, the lowest value of the tested range was set to 50 hr, while the highest value was set to 350 hr. The optimal combination of

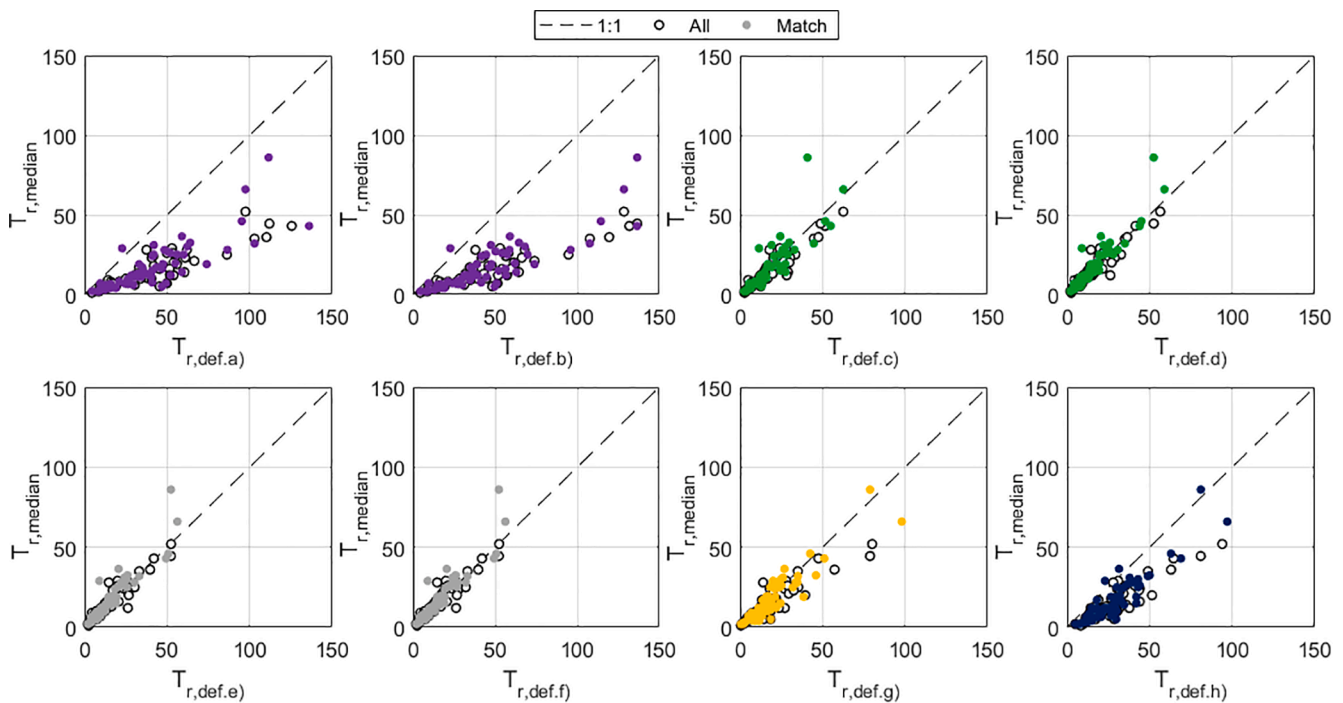


Fig. 7. Median values of the value set ($T_{r,median}$) resulting from the E-DMCA method (y-axis) compared to the median of the eight different T_r definitions [$T_{r,def. a-h)}$] from the SM method (x-axis). The medians are plotted for every selected events (All) and for those selected by both methods (Match). The definitions and the color codes correspond to those in Fig. 2.

Table 3

Goodness-of-fit measures of $T_{r,median}$ compared to the medians of the eight definitions [$T_{r,def. a-h}$] and the characteristic T_r ($T_{r,char}$). Values based on events selected by both the E-DMCA and SM methods are shown in parentheses.

	$T_{r,def. a}$	$T_{r,def. b}$	$T_{r,def. c}$	$T_{r,def. d}$	$T_{r,def. e}$	$T_{r,def. f}$	$T_{r,def. g}$	$T_{r,def. h}$	$T_{r,char}$
r [-]	0.906 (0.820)	0.911 (0.861)	0.937 (0.855)	0.940 (0.937)	0.942 (0.931)	0.938 (0.929)	0.886 (0.917)	0.896 (0.904)	0.967
NSE [-]	-0.427 (-0.233)	-0.468 (-0.246)	0.802 (0.603)	0.880 (0.750)	0.883 (0.746)	0.878 (0.755)	0.706 (0.817)	0.076 (0.353)	0.935
$RMSE$ [hr]	31.7 (29.5)	36.2 (33.8)	6.13 (7.94)	4.88 (6.03)	4.88 (6.17)	4.94 (6.10)	8.92 (7.13)	16.0 (13.8)	2.87
ΔT_r [%]	-63.8 (-58.4)	-66.4 (-61.7)	-18.7 (-5.96)	-1.77 (2.21)	-0.286 (1.52)	-1.67 (1.03)	-20.1 (-13.0)	-47.0 (-40.1)	0

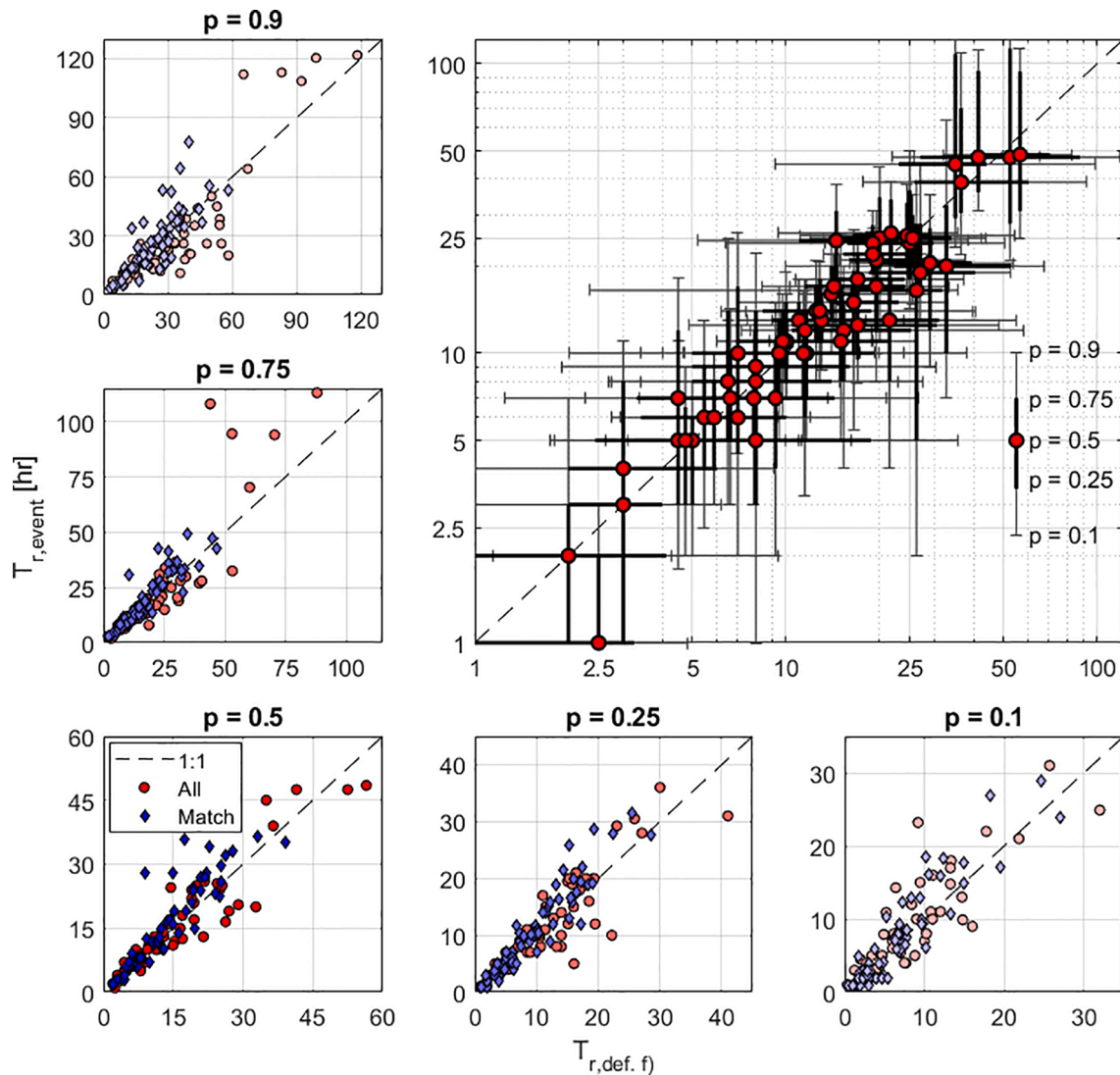


Fig. 8. Comparison of the different percentiles ($p = 0.1, 0.25, 0.5, 0.75, 0.9$) of T_r resulting from the E-DMCA method against those from the SM method using definition f). Percentiles based on all identified events are in red (All), while those from the same set of events (a subset of the former) among the two methods are in blue (Match). (For interpretation of the references to color in this figure legend, the reader is referred to the web version of this article.)

the two parameters ($T_{r,max}$ and p_{th}) was identified for all goodness-of-fit measures introduced in Section 3.4. The goodness-of-fit measures were calculated between the median of the T_r values yielded by the proposed method ($T_{r,median}$) and the median of the values resulting from definition f) [$T_{r,def. f}$]. The number of selected events per watershed per year was also calculated.

The sensitivity analysis demonstrates that the number of events selected with the E-DMCA approach only depends on the value of the threshold p_{th} [Fig. 9e)]. This was expected since the event selection relies on the fluctuations calculated using the characteristic T_r yielded by the DMCA method, which is not changing if the T_r 's value is higher than the characteristic T_r . However, the number of events selected increases

exponentially as the value of the threshold increases. A number of 20 events per watershed per year is reached near the value of $p_{th} = 0.05$, which can be considered a high value based on other studies (see Table 1). The value of $T_{r,max}$ has more effect on the set of event-based values, as it limits the upper part of the $T_{r,event}$'s distribution. This effect becomes clearly visible when the value of $T_{r,max}$ goes under 150 h, as all the goodness-of-fit measures show a sharp increase/decline when $T_{r,max} < 150$ hr and $p_{th} < 0.05$.

The different goodness-of-fit measures show somewhat different distributions for the two sets of catchments (see Section 3.4). The range of optimal $T_{r,max}$ goes from 75 to 150 h, and the value of optimal p_{th} is between 0.025 and 0.1. The optimum values match in the case of NSE

Table 4

Goodness-of-fit measures attributed to the different percentiles ($p = 0.1, 0.25, 0.5, 0.75, 0.9$) of T_r using the E-DMCA method and SM method with definition f). Values based on events selected by both methods are shown in parentheses.

p [-]	$T_{r,def. f} - T_{r,event}$				
	0.1	0.25	0.5	0.75	0.9
r [-]	0.875 (0.920)	0.900 (0.939)	0.938 (0.900)	0.887 (0.896)	0.900 (0.795)
NSE [-]	0.712 (0.746)	0.793 (0.757)	0.878 (0.641)	0.463 (0.702)	0.692 (0.282)
RMSE [hr]	3.32 (2.74)	3.62 (3.06)	4.94 (4.82)	12.0 (5.60)	12.9 (9.68)
ΔT_r [%]	7.00 (10.3)	-1.41 (2.31)	-1.67 (4.21)	5.78 (9.08)	-10.5 (8.15)

and RMSE [Fig. 9a & 9d]. ΔT_r yielded slightly different optima, while r resulted in considerably different optima [Fig. 9b & 9c]. However, r can be misleading since its value denotes a linear relationship and does not give information on the estimation error's extent. Consequently, the strongest linear relation between the modeled and estimated values does not necessarily coincide with the smallest estimation error. Based on the sensitivity analysis results displayed in Fig. 9, application of the parameter values $T_{r,max} = 150$ h, and $p = 0.05$ is considered well justified to run the E-DMCA method for the whole dataset.

5. Discussion

5.1. Comparison of event characteristics from different selection methods

Fig. 10 provides examples for the results of the event selection from the three different methods. Fig. 10a) demonstrates that the SM method is the most restrictive as it missed many of the events selected by the other two methods. Fig. 10b) provides examples for overlapping time windows in the case of the E-DMCA method. Overlaps between events also occur with the SBES method, but rarely. Fig. 10a) and 10b) represent two catchments with relatively short and long response times.

At some of the catchments, the SBES method failed to choose the largest observed flood events [Fig. 10c)], but in a few cases (5.5 % of the years) it selected a higher number of events than the other two methods [Fig. 10d)]. This suggest that the applied parameters of the SBES method should be calibrated individually for each catchment. The strongly variable performance of the three applied methods can be best observed in March and April of Fig. 10e). Fig. 10f-h) provide further examples for the various performance. The E-DMCA method was able to select more events than the SBES or both methods [Fig. 10f) & g), respectively]. Based on the results, selecting a few events by all three methods in one year, as in Fig. 10h), can be considered a relatively good match among the methods at this catchment.

The observed differences may stem from the different selection strategies of the applied methods. The general aim of the SM method was to provide a set of hydrologically reliable events through a strict selection procedure. This included the visual screening of the runoff events to

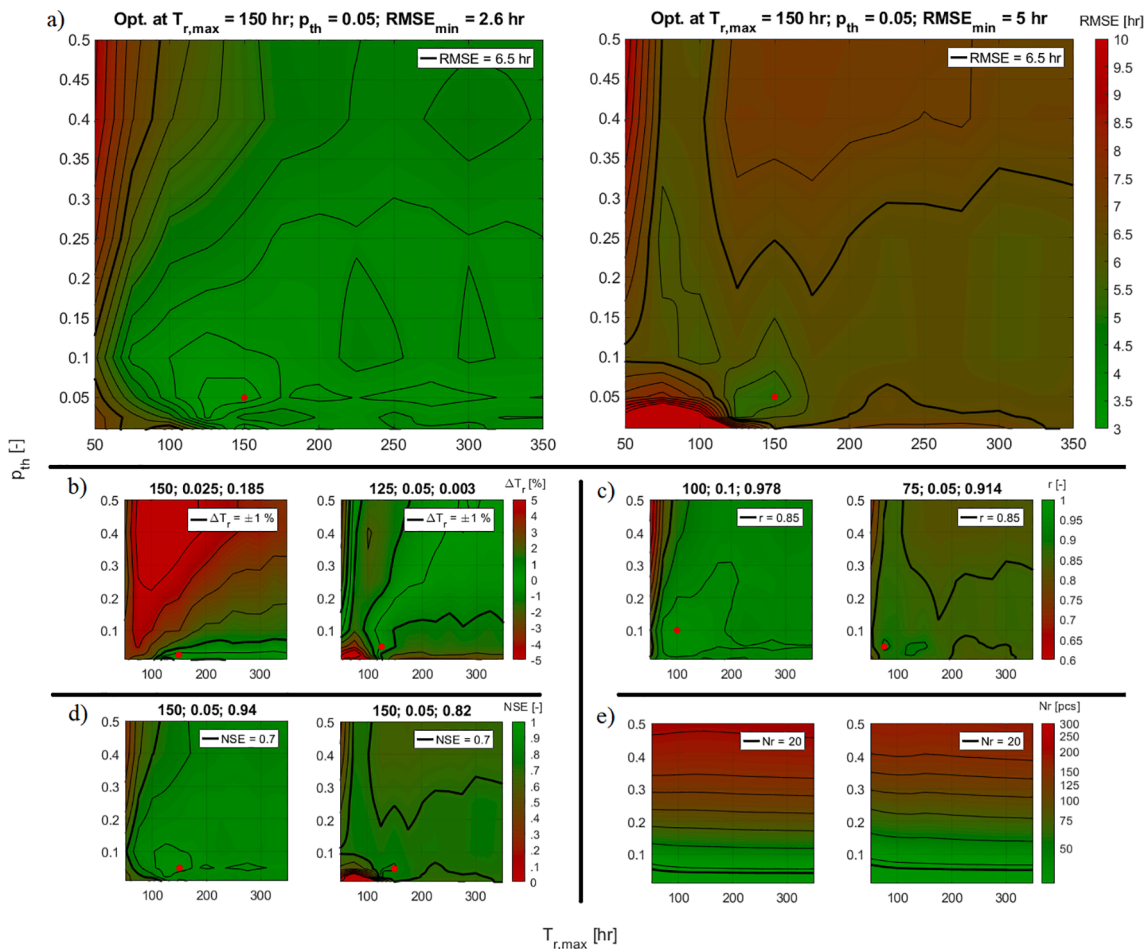


Fig. 9. Results of the sensitivity analysis in terms of the value of a) RMSE, b) ΔT_r , c) r , d) NSE, and e) the number of events (Nr) per watershed per year for catchment set #1 (left) and set #2 (right). The two subsets of catchments were created to perform a twofold cross-validation. They have the same size and were created by sorting the catchments into the subsets randomly.

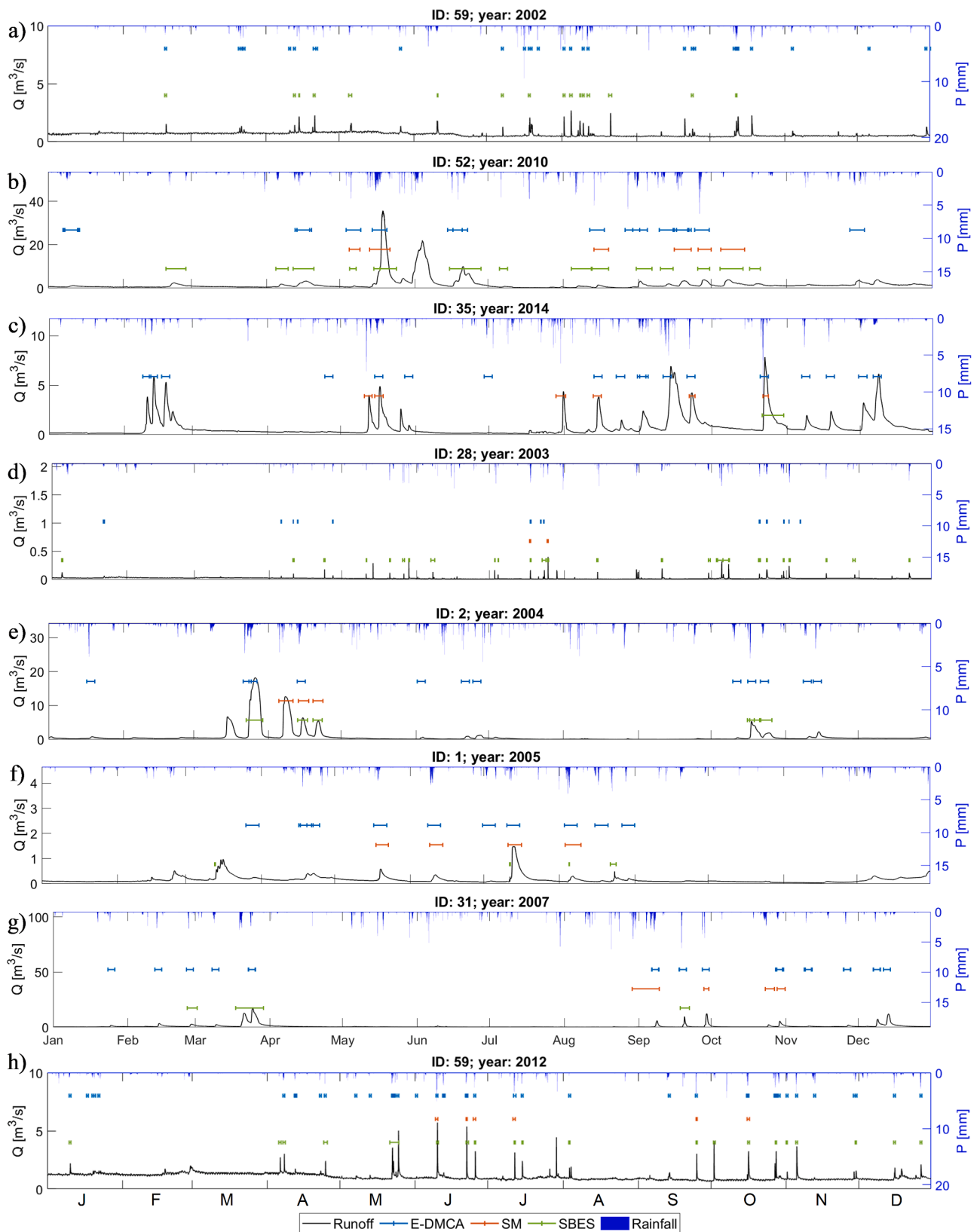


Fig. 10. Examples for event selection performance of the three applied methods. a) Catchment with short response time ($T_{r,median} = 6$ h) where SM fails to select events. b) Catchment with long response time ($T_{r,median} = 52$ h) where the E-DMCA method identifies overlapping time windows. c) Weak performance of the SBES method. d) The SBES method outperforms the SM and the E-DMCA methods. e) Varying performance of the three methods. f) Good match among the three methods. g) Good match between the SM and the E-DMCA methods. h) E-DMCA method selects more events than the SM and SBES methods. Catchment IDs correspond to those presented in Supplementary Material S1.

provide floods with a clear rising and recession limb lacking missing/interpolated values and measurement error, and the removal of events with less precipitation than direct runoff (see Section 3.1 for more details). This led to the exclusion of a large proportion (61.5 %) of the events, but this does not mean that these excluded events were falsely identified by the other two methods. Furthermore, the comparison of all selected events with the matched ones (Figs. 7 and 8) showed that the exclusion of these events does not result in a bias. In other words, a less strict selection strategy would lead to same results and the proposed method can provide a great number of reliable events for other hydrological analyses.

The SBES method relies on the variance of the runoff time-series which varies at different temporal resolutions. Since the SBES method was developed using daily time-series, the occasionally poor performance of the SBES method presented in this paper using hourly time-series could be further improved through a more extensive calibration of the method's numerous parameters. This means a re-calibration of the parameters for each catchment. Even though the runoff event selection could be likely enhanced as mentioned before, the runoff ratios would not necessarily improve since the SBES method does not account for the amount of rainfall attributed to the runoff events (in contrast to the E-DMCA and SM methods).

The E-DMCA method fails to identify some of the events due to two main reasons: a) the event is identified, but it is ill-conditioned (see Section 3.3), or; b) the corresponding precipitation arrives too early/late or is quantitatively insufficient (i.e., the selection criteria introduced in Section 3.3 is not fulfilled). Despite these cases, the E-DMCA method appeared to perform well, as discussed in the following sections.

Regarding the runoff ratios, the SM and E-DMCA values showed the strongest correlation, while the values from the SBES method showed little agreement with the values yielded by the other two (SM and E-DMCA) methods. The values were also plotted using every selected event and only for the events selected by the two compared methods (see Supplementary Material S2, Sections 1 and 2). The runoff ratios resulting from the SBES method show stronger correlation with the values yielded by the SM method when only the matching events are compared. The difference between examining all events and only the matching events is not notable when comparing the E-DMCA and SM methods. This means to us that in contrast to the E-DMCA method, the further selected events by the SBES method may not be reliable and a visual inspection would be necessary. This is a clear disadvantage in the case of an automated method. The SBES method's values generally overestimate the runoff ratios resulting from the E-DMCA method (see Fig. 5), and the overestimation grows more significant as the percentile decreases.

The above mentioned discrepancies can be attributed again to the selection strategies of the different methods. The SM method employs several strict and arbitrary criteria in order to produce a smaller but hydrologically reliable set of rainfall-runoff events. Since the SM method requires the separation of base flow and effective precipitation, leading to the exclusion of events with less precipitation than direct runoff, its results can be considered the most reliable. An important aspect of the SBES method is that it does not consider the volume of the precipitation, therefore it does not ensure that the amount of the attributed rainfall is sufficient to produce the identified runoff. This could lead to the larger differences between the values of the SM and SBES methods when comparing every selected event instead of matching events. The E-DMCA method builds upon both the rainfall and the runoff fluctuation time-series, meaning the method cannot select a runoff event if there is no precipitation (or the precipitation is too small to produce fluctuation above p_{th}). This may result in the stronger correlation between the SM and E-DMCA methods.

Considering the T_r values resulting from the different methods, the SBES and E-DMCA methods exhibit the strongest correlation. In contrast, the T_r values yielded by the SM method are somewhat longer than the T_r resulting from the other two (SBES and E-DMCA) methods.

This can be attributed to two main factors. First, the number of matching events is very low (0.871 and 1.76 events per catchment per year on average) between the SM and the other two methods (for more details, see Supplementary Material S2, Section 3). If some of these events are not well defined (i.e., the beginning and/or the end of the event is mispositioned), the resulting T_r can be easily distorted. Second, the SM method defines longer time windows for the events than the other two event selection methods. This can lead to longer T_r values after the application of the DMCA method.

Based on the comparative analysis of the α and T_r values, the events selected by the proposed E-DMCA method appears to be appropriate. When considering the time requirements to evaluate the SM, SBES, and E-DMCA methods, they can yield results in days, hours, and minutes, respectively. Furthermore, the proposed E-DMCA method employs only two parameters, while the SBES method requires nine. These properties of the proposed method underline that the E-DMCA method is the most efficient tool to assess an event-based set of T_r values from rainfall and runoff time-series. A more detailed assessment of additional event characteristics (e.g., event duration, ratio of peak discharge to base flow, etc.) could highlight further strengths and weaknesses of the examined methods. The evaluation of other available event selection methods (see Table 1) could reveal further insights of the different approaches of event selection.

5.2. Evaluation of the various catchment response times resulting from the SM and E-DMCA methods

The E-DMCA method yielded satisfactory results in every examined aspect. The median of $T_{r,event}$ matched the characteristic T_r estimated with the original method of Giani et al. (2021) quite well ($RMSE = 2.87$ hr). Since the DMCA T_r estimation method can only yield integers for hourly time-series, the relative error can be high for smaller catchments with shorter T_r . Using a shorter time-step for smaller catchments could produce a better estimation in these cases.

Application of the different T_r definitions resulted in theoretically plausible relations. Definitions c)-f) gave the best results with only slight differences ($RMSE = 6.13-4.88$ hr). The DMCA method defines the time between the centroids of total rainfall and streamflow, but it tends to give more weight to higher peaks (Giani et al., 2021). As we tested the original DMCA T_r estimation method, we also found that it appears to match the peaks of the observed rainfall and runoff time-series in the case of multi-peaked events. This is especially true when the rainfall and streamflow peak is close to each other, i.e., the last peak of the rainfall and the first peak of the streamflow are the largest ones. For this reason, we aimed to test the efficiency of the E-DMCA method against definition f). However, the relatively small difference in performance among definitions c)-f) implies that this choice did not affect the efficiency of the proposed method considerably.

By definition, T_c is calculated based on velocity, while T_e is calculated based on celerity (Beven, 2020). Since celerity is normally higher than velocity (Beven, 2020), the value of T_c is expected to be larger than the value of T_e . In fact, T_c 's value can be considered an upper limit of catchment response time (Giani et al., 2021). Even though Giani et al. (2021) used definition a) to calculate T_r for the selected events in their study, their results showed a 1:1 match between the characteristic T_r calculated with the original DMCA method, and the median of the values assessed using definition a). However, the results presented in this study are more plausible, since the DMCA method should yield a value closer to T_L by nature, and T_L must be shorter, than T_c , based on their definitions.

For a deeper understanding of the connection between the various time parameters, we attributed different percentiles of the $T_{r,event}$ values resulting from the E-DMCA method to the median values of definitions [a), f), g), and h)]. Fig. 11 displays the value of $RMSE$ in relation to the different percentiles of $T_{r,event}(p)$ along with the best fit for definitions a), f), g), and h) for the events selected by both methods. For example, the

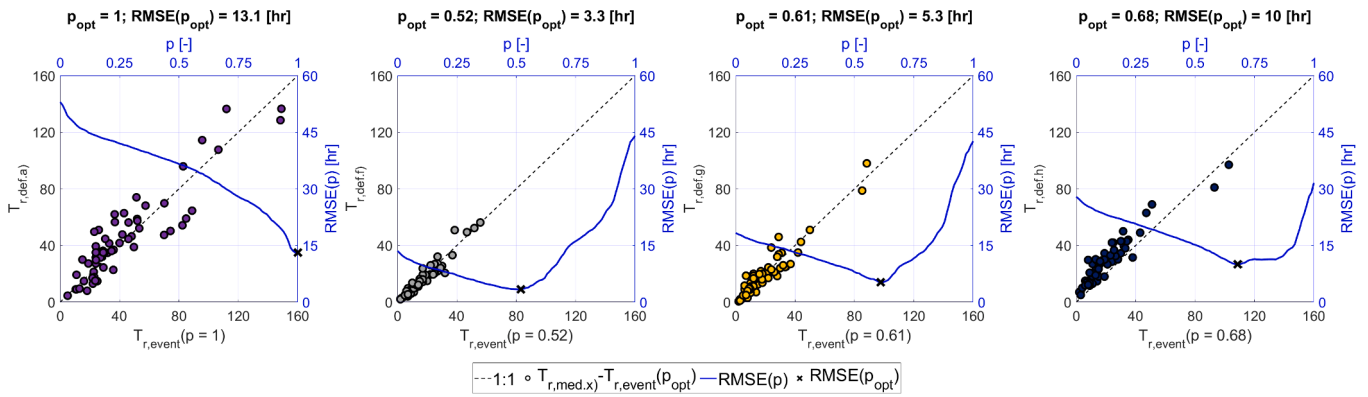


Fig. 11. Estimating the median of definition a), f), g) and h) by recalibrating the corresponding percentiles (p) of $T_{r,event}$. The secondary (blue) x-axis shows the percentile (p), while the secondary (blue) y-axis shows the $RMSE$ value between $T_{r,def. x}$ and $T_{r,event}(p)$. (For interpretation of the references to color in this figure legend, the reader is referred to the web version of this article.)

$RMSE$ is the lowest near $p = 0.5$ in the case of definition f) since the E-DMCA method was optimized to the median of definition f). The characteristic value of T_c can be estimated by picking the maximum of the $T_{r,event}$ values resulting from the E-DMCA approach at a satisfactory level ($RMSE = 13.1$ hr). This is reasonable, since T_c can be considered an upper limit of a catchment's T_r by definition. The median of T_p can also be estimated as the $p = 0.61$ percentile of $T_{r,event}$ with $RMSE = 5.30$ hr. However, the value of T_e was assessed with much lower precision ($RMSE = 10.0$ hr). Nevertheless, the range of these time parameters increase in the expected order, namely: $T_c > T_e > T_p > T_L$.

In addition to the work of Giani et al. (2021), the E-DMCA method presented in this paper managed to assess different percentiles of the T_r distribution at a satisfactory level ($RMSE = 3.32$ – 12.9 hr). It cannot be undoubtedly decided which event selection method gives more realistic results since there is no unified method to collect rainfall-runoff events. The SM method involves arbitrary choices, which makes the process less objective and unreproducible. The proposed method is more of a stochastic approach, since it collects rainfall-runoff events based on probability through the parameter p_{th} . This method produces a set of values including a higher number of the extremely short and long T_r values, which results in the observed differences. However, the E-DMCA method is able to capture the variable nature of T_r and yields its distribution in minutes.

5.3. Sensitivity analysis

Based on the sensitivity analysis results, the parameters $T_{r,max} = 150$ hr, and $p_{th} = 0.05$ can be used for similar catchments and identical climatic conditions. The analysis illustrated that it is safer to overestimate the value of $T_{r,max}$, than to underestimate it, since $T_{r,max}$ is the upper boundary of the event-based set of values. If $T_{r,max}$ is underestimated it leads to a sharp decrease in the performance of the E-DMCA method (see Section 4.3, Fig. 9). The estimation error does not vary considerably in the range of $p_{th} = 0.01$ – 0.05 when $T_{r,max} \geq 150$ hr. The value of $T_{r,max}$ matched the maximum of the values defined using definition f) and approximately equals three times the maximum of the characteristic T_r values yielded by the original DMCA method. Therefore, we suggest two methods to estimate $T_{r,max}$: a) assess $T_{r,max}$ manually from the time-series of the largest catchment by finding the longest response; b) perform the original DMCA method for long time-series then choose $T_{r,max}$ equal to or greater than the triple of the longest characteristic T_r . To keep the number of selected events under an average of 20 events per catchment per year, we suggest using a value of p_{th} smaller than 0.05. However, the number of selected events can strongly vary across different climatic regions, applied methods and criteria (see Table 1). Therefore, the values of p_{th} can be adjusted to the specific conditions and requirements.

The parameter values suggested above could be used for similar

catchments, making the evaluation of the event selection externally dispensable. However, the method should be tested on a larger, more variable set of catchments in order to extend the applicability of the E-DMCA method and assess the robustness of the two parameters in more detail. The SM method could be performed more sufficiently using only definition f) for a larger dataset since the separation of effective rainfall and direct runoff is not necessary in this case.

6. Conclusions

The E-DMCA method presented in this study was able to select rainfall-runoff events to estimate the range of possible T_r values in the case of 61 medium-sized Hungarian catchments. The following conclusions can be drawn from the performed analysis:

- The E-DMCA method is capable of selecting events from long time-series and yield an event-based set of T_r values ($T_{r,event}$) in an automated fashion, thus effectively obliterating days of work normally required to perform a non-automated approach.
- Based on the results of the sensitivity analysis, an optimal range/value was identified for the two parameters (p_{th} and $T_{r,max}$) needed to perform the presented method (see Section 3.3). The range for p_{th} is 0.01–0.05, while the value of $T_{r,max}$ can be estimated as triple the maximum of the characteristic T_r values resulting from the application of the original DMCA method on long time-series.
- Compared to the values resulting from the different graphical definitions, the T_r values of the new method are the closest to the time elapsed between the peaks of the total rainfall and runoff. In addition, the characteristic value of T_c can be estimated as the maximum of the event-based set of values ($T_{r,event}$) yielded by the E-DMCA method.
- The application of the event selection method of Fischer et al. (2021) highlighted that the rainfall-runoff events identified by the E-DMCA method are hydrologically reliable considering rainfall-runoff ratios. This is due to the fact that the E-DMCA method cannot select a runoff event if there is no sufficient preceding precipitation, while the method of Fischer et al. (2021) does not consider the amount of rainfall.
- It was also demonstrated that the proposed method is easier to implement as it has only two parameters instead of nine. This is especially true at the hourly temporal resolution, since the runtime of the E-DMCA method is considerably shorter. The added value of the proposed method is that it yields a range of physically possible values (instead of a characteristic value per watershed) in one step and within minutes. This is an important step toward future implementation of modeling non-linear and stochastic catchment behavior in everyday engineering/hydrological applications.

The proposed E-DMCA method yielded promising results assessed by the runoff ratio and catchment response time. The authors intend to broaden the analysis of the proposed method in the future with regard to the number of i) event selection methods tested; ii) rainfall-runoff event characteristics assessed; iii) catchments examined, and; iv) temporal resolution investigated, which could further contribute in general to the hydrological analysis and modeling of rainfall-runoff events.

CRedit authorship contribution statement

Eszter D. Nagy: Conceptualization, Methodology, Software, Formal analysis, Investigation, Data curation, Writing – original draft, Visualization. **Jozsef Szilagyi:** Writing – review & editing, Supervision. **Peter Torma:** Writing – review & editing, Supervision.

Declaration of Competing Interest

The authors declare that they have no known competing financial interests or personal relationships that could have appeared to influence the work reported in this paper.

Data availability

The authors do not have permission to share data. The code is shared at <https://doi.org/10.5281/zenodo.6822134>.

Acknowledgments

This research, carried out at the Budapest University of Technology and Economics, was supported by the “TKP2020, Institutional Excellence Program” of the National Research, Development and Innovation (NRDI) Office in the field of Water Sciences & Disaster Prevention (BME IE-VIZ TKP2020). Additional support was provided by the Ministry of Innovation and Technology of Hungary from the National Research, Development and Innovation Fund, financed under the TKP2021 funding scheme (project# BME-NVA-02). Partial support by the ÚNKP-20-3 new national excellence program of the Ministry for Innovation and Technology from the NRDI Fund and the data service of the local Water Directorates are also gratefully acknowledged. The authors are grateful for the useful suggestions of two anonymous reviewers. The changes made based on their comments greatly improved this article.

Data statement.

Data supporting this research can be requested through <http://www.ovf.hu/en/vizrajzi-adatok-en> from the General Directorate of Water Management. The data are available only for research purposes at governmental institutions in Hungary and are not accessible to the public or international research community. The code for the E-DMCA method (Nagy, 2022) is freely available at <https://doi.org/10.5281/zenodo.6822134>.

Appendix A. Supplementary data

Supplementary data to this article can be found online at <https://doi.org/10.1016/j.jhydrol.2022.128355>.

References

Abdel-Fattah, M., Saber, M., Kantoush, S.A., Khalil, M.F., Sumi, T., Sefelnasr, A.M., 2017. Hydrological and Geomorphometric Approach to Understanding the Generation of Wadi Flash Floods. *Water* 9 (7), 553. <https://doi.org/10.3390/w9070553>.

Amiri, B.J., Gao, J., Fohrer, N., Adamowski, J., Huang, J., 2019. Examining lag time using the landscape, pedoscape and lithoscape metrics of catchments. *Ecol. Ind.* 105, 36–46. <https://doi.org/10.1016/j.ecolind.2019.03.050>.

Azizian, A., 2019. Comparison of salt experiments and empirical time of concentration equations. *Proc. Inst. Civ. Eng. - Water Manage.* 172 (3), 109–122. <https://doi.org/10.1680/jwama.17.00048>.

Baiamonte, G., Singh, V.P., 2016. Analytical solution of kinematic wave time of concentration for overland flow under green-ampt infiltration. *J. Hydrol. Eng.* 21 (3), 1–17. [https://doi.org/10.1061/\(ASCE\)HE.1943-5584.0001266](https://doi.org/10.1061/(ASCE)HE.1943-5584.0001266).

Beven, K.J., 2012. In: *Rainfall-runoff modelling: the primer*. Wiley-Blackwell. <https://doi.org/10.1002/9781119951001>.

Beven, K.J., 2020. A history of the concept of time of concentration. *Hydrol. Earth Syst. Sci.* 24, 2655–2670. <https://doi.org/10.5194/hess-24-2655-2020>.

Black, P.E., 1972. Hydrograph Response to Geomorphic Model Watershed Characteristics and Precipitation Variables. *J. Hydrol.* 17 (4), 309–329. [https://doi.org/10.1016/0022-1694\(72\)90090-X](https://doi.org/10.1016/0022-1694(72)90090-X).

Bondelid, T.R., McCuen, R.H., Jackson, T.J., 1982. Sensitivity of SCS Models to Curve Number Variation. *JAWRA Journal of the American Water Resources Association* 18 (1), 111–116. <https://doi.org/10.1111/j.1752-1688.1982.tb04536.x>.

Chow, V.T., Maidment, D.R., Mays, L.W., 1988. *Applied hydrology*. McGraw Hill, New York.

Copernicus Climate Change Service (C3S), 2019. C3S ERA5-Land reanalysis. Copernicus Climate Change Service. 2019 (08), 16.

Copernicus, L.M.S., (2016). *European Digital Elevation Model (EU-DEM), version 1.1*. <https://land.copernicus.eu/imagery-in-situ/eu-dem/eu-dem-v1.1> (accessed 14 July 2019).

Copernicus, L.M.S., (2020a). *Tree Cover Density 2018*. <https://land.copernicus.eu/pan-european/high-resolution-layers/forests/tree-cover-density/status-maps/tree-cover-density-2018> (accessed 5 September 2020).

Copernicus, L.M.S., (2020b). *Imperviousness Density 2018*. <https://land.copernicus.eu/pan-european/high-resolution-layers/imperviousness/status-maps/imperviousness-density-2018> (accessed 5 September 2020).

Cuevas, J.G., Arumí, J.L., Dörner, J., 2019. Assessing methods for the estimation of response times of stream discharge: The role of rainfall duration. *Journal of Hydrology and Hydromechanics* 67 (2), 143–153. <https://doi.org/10.2478/johh-2018-0043>.

Dingman, S.L., 2015. *Physical Hydrology (Third)*. IL, Waveland Press, Long Grove.

Fang, X., Thompson, D.B., Cleveland, T.G., Pradhan, P., Malla, R., 2008. Time of concentration estimated using watershed parameters determined by automated and manual methods. *J. Irrig. Drain. Eng.* 134 (2), 202–211. [https://doi.org/10.1061/\(ASCE\)0733-9437\(2008\)134:2\(202\)](https://doi.org/10.1061/(ASCE)0733-9437(2008)134:2(202)).

Fischer, S., Schumann, A., Bühler, P., 2021. A statistics-based automated flood event separation. *Journal of Hydrology X* 10, 100070. <https://doi.org/10.1016/j.hydroa.2020.100070>.

Gaál, L., Szolgay, J., Kohnová, S., Parajka, J., Merz, R., Viglione, A., Blöschl, G., 2012. Flood timescales: Understanding the interplay of climate and catchment processes through comparative hydrology. *Water Resour. Res.* 48 (4) <https://doi.org/10.1029/2011WR011509>.

Gericke, O.J., Smithers, J.C., 2017. Direct estimation of catchment response time parameters in medium to large catchments using observed streamflow data. *Hydrol. Process.* 31 (5), 1125–1143. <https://doi.org/10.1002/hyp.11102>.

Giani, G., Rico-Ramirez, M.A., Woods, R.A., 2021. A Practical, Objective, and Robust Technique to Directly Estimate Catchment Response Time. *Water Resour. Res.* 57 (2) <https://doi.org/10.1029/2020WR028201>.

Grimaldi, S., Petroselli, A., Tauro, F., Porfiri, M., 2012. Time of concentration: a paradox in modern hydrology. *Hydrol. Sci. J.* 57 (2), 217–228. <https://doi.org/10.1080/02626667.2011.644244>.

Institute of Hydrology, 1999. *Flood Estimation Handbook (FEH) (5 volumes)*. Wallingford, UK.

Kaufmann de Almeida, I., Kaufmann Almeida, A., Garcia Gabas, S., Alves Sobrinho, T., 2017. Performance of methods for estimating the time of concentration in a watershed of a tropical region. *Hydrol. Sci. J.* 62 (14), 2406–2414. <https://doi.org/10.1080/02626667.2017.1384549>.

Khanal, P.C., 2004. *Development of regional synthetic unit hydrograph for Texas watersheds*. Lamar University, Beaumont, Texas.

Kjeldsen, T.R., Kim, H., Jang, C.-H., Lee, H., 2016. Evidence and Implications of Nonlinear Flood Response in a Small Mountainous Watershed. *J. Hydrol. Eng.* 21 (8) [https://doi.org/10.1061/\(ASCE\)HE.1943-5584.0001343](https://doi.org/10.1061/(ASCE)HE.1943-5584.0001343).

Koskelo, A.I., Fisher, T.R., Utz, R.M., Jordan, T.E., 2012. A new precipitation-based method of baseflow separation and event identification for small watersheds (<50 km²). *J. Hydrol.* 450–451, 267–278. <https://doi.org/10.1016/J.JHYDROL.2012.04.055>.

Langridge, M., Gharabaghi, B., McBean, E.d., Bonakdari, H., Walton, R., 2020. Understanding the dynamic nature of Time-to-Peak in UK streams. *J. Hydrol.* 583, 124630.

Liang, J., Melching, C.S., 2012. Comparison of computed and experimentally assessed times of concentration for a V-shaped laboratory watershed. *J. Hydrol. Eng.* 17 (12), 1389–1396. [https://doi.org/10.1061/\(ASCE\)HE.1943-5584.0000609](https://doi.org/10.1061/(ASCE)HE.1943-5584.0000609).

Loukas, A., Quick, M.C., 1996. Physically-based estimation of lag time for forested mountainous watersheds. *Hydrol. Sci. J.* 41 (1), 1–19. <https://doi.org/10.1080/02626669609491475>.

Mathias, S.A., McIntyre, N., Oughton, R.H., 2016. A study of non-linearity in rainfall-runoff response using 120 UK catchments. *J. Hydrol.* 540, 423–436. <https://doi.org/10.1016/J.JHYDROL.2016.06.039>.

McCuen, R.H., 2009. Uncertainty Analyses of Watershed Time Parameters. *J. Hydrol. Eng.* 14 (5), 490–498. [https://doi.org/10.1061/\(ASCE\)HE.1943-5584.0000011](https://doi.org/10.1061/(ASCE)HE.1943-5584.0000011).

Mei, Y., Anagnostou, E.N., 2015. A hydrograph separation method based on information from rainfall and runoff records. *J. Hydrol.* 523, 636–649. <https://doi.org/10.1016/j.jhydrol.2015.01.083>.

Merz, R., Blöschl, G., 2009. A regional analysis of event runoff coefficients with respect to climate and catchment characteristics in Austria. *Water Resour. Res.* 45, W01405. <https://doi.org/10.1029/2008WR007163>.

- Meyersohn, W.D., 2016. Runoff Prediction for Dam Safety Evaluations Based on Variable Time of Concentration. *J. Hydrol. Eng.* 21 (10), 04016031. [https://doi.org/10.1061/\(ASCE\)HE.1943-5584.0001406](https://doi.org/10.1061/(ASCE)HE.1943-5584.0001406).
- Michailidi, E.M., Antoniadis, S., Koukouvinos, A., Bacchi, B., Efstratiadis, A., 2018. Timing the time of concentration: shedding light on a paradox. *Hydrol. Sci. J.* 63 (5), 721–740. <https://doi.org/10.1080/02626667.2018.1450985>.
- Minshall, N.E., 1960. Predicting storm runoff on small experimental watersheds. *J. Hydraul. Div. ASCE* 86 (HY8), 17–38.
- Nagy, E. D. (2022, July 12). Tr_DMCA_eventbased: Original Release (Version v1.0). Zenodo. <https://doi.org/10.5281/zenodo.6822134>.
- Nagy, E.D., Szilágyi, J., 2020. Comparative analysis of catchment response times and their definitions using measured and re-analysis rainfall data. *HydroCarpath International Conference: Processes, Patterns and Regimes in the Hydrology of the Carpathians: Coupling Experiments, Remote Sensing, Citizen. Science* 9. <https://doi.org/10.13140/RG.2.2.29763.02089>.
- Nagy, E.D., Szilágyi, J., 2021. Revision of Wisnovszky's equation by a comprehensive analysis of measured time of concentration and catchment morphological parameter values (in Hungarian). *Hungarian J. Hydrol.* 101 (1), 19–32. http://www.hidrologia.hu/mht/letoltes/HK2021_01_v4.pdf.
- Nagy, E.D., Torma, P., Bene, K., 2016. Comparing Methods for Computing the Time of Concentration in a Medium-Sized Hungarian Catchment. *Slovak J. Civ. Eng.* 24 (4), 8–14. <https://doi.org/10.1515/sjce-2016-0017>.
- Nash, J.E., Sutcliffe, J.V., 1970. River flow forecasting through conceptual models part I – A discussion of principles. *J. Hydrol.* 10 (3), 282–290. [https://doi.org/10.1016/0022-1694\(70\)90255-6](https://doi.org/10.1016/0022-1694(70)90255-6).
- Nathan, R.J., McMahon, T.A., 1990. Evaluation of automated techniques for base flow and recession analyses. *Water Resour. Res.* 26 (7), 1465–1473. <https://doi.org/10.1029/WR026i007p01465>.
- Norbiato, D., Borga, M., Merz, R., Blöschl, G., Carton, A., 2009. Controls on event runoff coefficients in the eastern Italian Alps. *J. Hydrol.* 375, 312–325. <https://doi.org/10.1016/j.jhydrol.2009.06.044>.
- Oppel, H., Mewes, B., 2020. On the Automation of Flood Event Separation From Continuous Time Series. *Front. Water* 2 (July), 1–14. <https://doi.org/10.3389/frwa.2020.00018>.
- Peel, M.C., Finlayson, B.L., McMahon, T.A., 2007. Updated world map of the Köppen-Geiger climate classification. *Hydrol. Earth Syst. Sci.* 11, 1633–1644. <https://doi.org/10.5194/hess-11-1633-2007>.
- Pilgrim, D.H., 1976. Travel times and nonlinearity of flood runoff from tracer measurements on a small watershed. *Water Resour. Res.* 12 (3), 487–496. <https://doi.org/10.1029/WR012i003p00487>.
- Ravazzani, G., Boscarello, L., Cislighi, A., Mancini, M., 2019. Review of Time-of-Concentration Equations and a New Proposal in Italy. *J. Hydrol. Eng.* 24 (10), 1–11. [https://doi.org/10.1061/\(ASCE\)HE.1943-5584.0001818](https://doi.org/10.1061/(ASCE)HE.1943-5584.0001818).
- Reed, D.W., Johnson, P., Firth, J.M., 1975. A non-linear rainfall-runoff model, providing for variable lag time. *J. Hydrol.* 25 (3–4), 295–305. [https://doi.org/10.1016/0022-1694\(75\)90027-X](https://doi.org/10.1016/0022-1694(75)90027-X).
- Rodriguez, N.B., Pfister, L., Zehe, E., Klaus, J., 2021. A comparison of catchment travel times and storage deduced from deuterium and tritium tracers using StorAge Selection functions. *Hydrol. Earth Syst. Sci.* 25 (1), 401–428.
- Sabzevari, T., Noroozpour, S., Pishvaei, M.H., 2015. Effects of geometry on runoff time characteristics and time-area histogram of hillslopes. *J. Hydrol.* 531, 638–648. <https://doi.org/10.1016/j.jhydrol.2015.10.063>.
- Saghafian, B., Julien, P.Y., Rajaie, H., 2002. Runoff hydrograph simulation based on time variable isochrone technique. *J. Hydrol.* 261 (1–4), 193–203. [https://doi.org/10.1016/S0022-1694\(02\)00007-0](https://doi.org/10.1016/S0022-1694(02)00007-0).
- Sauquet, E., Catalogne, C., 2011. Comparison of catchment grouping methods for flow duration curve estimation at ungauged sites in France. *Hydrol. Earth Syst. Sci.* 15, 2421–2435. <https://doi.org/10.5194/hess-15-2421-2011>.
- Strahler, A.N., 1957. Quantitative analysis of watershed geomorphology. *Eos, Transactions American Geophysical Union* 38 (6), 913–920. <https://doi.org/10.1029/TR038i006p00913>.
- Szilágyi, J., 2007. Analysis of the nonlinearity in the hillslope runoff response to precipitation through numerical modeling. *J. Hydrol.* 337, 391–401. <https://doi.org/10.1016/J.JHYDROL.2007.02.005>.
- Szilágyi, J., Harvey, F.E., Ayers, J.F., 2003. Regional Estimation of Base Recharge to Ground Water Using Water Balance and a Base-Flow Index. *Ground Water* 41 (4), 504–513. <https://doi.org/10.1111/j.1745-6584.2003.tb02384.x>.
- Tarasova, L., Basso, S., Zink, M., Merz, R., 2018. Exploring Controls on Rainfall-Runoff Events: 1 Time Series-Based Event Separation and Temporal Dynamics of Event Runoff Response in Germany. *Water Resour. Res.* 54 (10), 7711–7732. <https://doi.org/10.1029/2018WR022587>.
- Thiesen, S., Darscheid, P., Ehret, U., 2019. Identifying rainfall-runoff events in discharge time series: a data-driven method based on information theory. *Hydrol. Earth Syst. Sci.* 23, 1015–1034. <https://doi.org/10.5194/hess-23-1015-2019>.
- W.M.O. (1974). International Glossary of Hydrology, W.M.O. Report No. 385: Geneva.
- Wisnovszky, I., 1958. *The Computation of the Time of Concentration (in Hungarian)*. *Hungarian J. Hydrol.* 3, 195–200.
- Wu, S.J., Yeh, K.C., Ho, C.H., Yang, S.H., 2016. Modeling probabilistic lag time equation in a watershed based on uncertainties in rainfall, hydraulic and geographical factors. *Hydrol. Res.* 47 (6), 1116–1141. <https://doi.org/10.2166/nh.2016.134>.
- Zhang, S., Liu, C., Yao, Z., Guo, L., 2007. Experimental study on lag time for a small watershed. *Hydrol. Process.* 21 (8), 1045–1054. <https://doi.org/10.1002/hyp.6285>.